Phosphorus (III) Tricationic and Dicationic Complexes

by

Hannah Christine Sinclair
BSc., Acadia University, 2015

A Thesis Submitted in Partial Fulfillment
of the Requirements for the Degree of

MASTER OF SCIENCE

in the Department of Chemistry

Phosphorus (III) Tricationic and Dicationic Complexes

by

Hannah Christine Sinclair
BSc., Acadia University, 2015

Supervisory Committee

Dr. Neil Burford, Supervisor
(Department of Chemistry, University of Victoria)

Dr. Lisa Rosenberg, Departmental Member
(Department of Chemistry, University of Victoria)

ABSTRACT

Supervisory Committee

Dr. Neil Burford, Supervisor

(Department of Chemistry, University of Victoria)

Dr. Lisa Rosenberg, Departmental Member

(Department of Chemistry, University of Victoria)

Coordination chemistry usually applies to transition metals, but has recently been extended to the *p*-block elements. For the pnictogen atoms (group 15), this type of coordination chemistry has already been applied to antimony and bismuth, where they behave as Lewis acceptor centres. However, complexes with nitrogen and phosphorus as Lewis acidic centres are rare, due to their relatively small atomic radii and inherent basic nature. Instead, these elements (Pn(III)) are typically observed as donor centres because they are better at donating their electron pair, than they are at accepting them. To enhance the Lewis acidity at the phosphorus and nitrogen centres, a cationic charge can be introduced by heterolytically abstracting a halide and replacing it with a weakly coordinating anion, providing more opportunities for new reactivity. The presence of a stereochemically active lone pair at the acceptor site also introduces new reactivity patterns to be explored. The formation of these main group coordination complexes opens doors to potential applications in catalysis, small molecule activation, or as material precursors. 2,2'-bipyridine (bipy) has been a prototypical ligand used in transition metal coordination chemistry due to its high basicity and oxidative resistance. This property has been exploited to enable a comprehensive study of a series of Pn(III) tricationic and dicationic complexes using 2,2'-bipyridine (bipy); 4,4'-di-tert-butyl-2,2'-bipyridine ($^{t}Bu_2$bipy); 4-dimethylaminopyridine (DMAP); and other main group containing ligands.

Table of Contents

List of Figures

List of Schemes

List of Tables

Acknowledgements

First and foremost, I am greatly indebted to Professor Neil Burford. With his constant support, humour, and "keep doing what you're doing" attitude, Neil made grad school possible and made these last two years at UVic an amazing experience. It wouldn't matter what I wanted to talk about, Neil was there to listen, to advise, and to offer tea (or some other beverage). His advice has helped me more times than I can count and has shaped me as an individual, and for that I am deeply thankful.

I am grateful for the financial support from the Natural Sciences and Engineering Research Council of Canada. It's amazing that I can obtain a MSc degree and not have to hold down a full-time job to pay for it. The greatest jobs are the ones where you can learn and get paid, and for that, I am thankful for NSERC's support.

I would like to thank Dr. Robert McDonald and Dr. Michael J. Ferguson at the University of Alberta and Dr. Brian Patrick at the University of British Columbia for their unwavering ability in obtaining workable crystal data from the samples I sent them. Without their help with solving crystal structures, my thesis would be very different (and boring).

My two years at UVic would not have been filled with as many laughs had I not been surrounded by these outstanding people: Paul Gray, Chris Frazee, Max Poller, Riccardo Suter, the number of exchange students and undergraduates, as well as honorary member, and best friend, Leah Gajecki. Without their constant support with research, writing, presentations, and posters, (not to mention drinking sessions), my experience at UVic would have only been a shell. To you, and to all the other amazing people at UVic I am now privileged to call friends, thank you. The friendships I have made in these short years are strong enough to last a lifetime, and I wish you all the best with your PhDs and careers. I am *deeply* indebted to your kindness and especially your patience. I owe you all some Advil for two years of headaches.

It's tough moving across the country to pursue a graduate degree, but it would have been more challenging if I did not have the unwavering support of my family back in Nova Scotia. I especially would like to thank my twin sister, Jessie, who made the big move away from home with me, and although it wasn't for long, the transition was a lot easier. My family continuously provided me with support with numerous phone and skype calls, snail mail, and, of course, with *unforgettable* visits; I love you all so very much.

However, whenever I needed to vent about chemistry problems, grad school problems… and just about any other problem you could think of, I could always count on Dr. Bobby Ellis and his amazing wife Tracy Murray to help me through it. I can honestly say that without you, I would not be here, nor would I be the person I am today. You made all this possible; thank you for everything.

Finally, I would like to thank David Maguire. My life has never stood still, but you've always kept me grounded. I cannot thank you enough for your love and support these past two years. I promise to stop coming home smelling like the lab.

List of Abbreviations and Symbols

Å	Angstrom
BIAN	*bis*(aryl-imino)acenaphthene
$BimEt_3$	1-ethyl-*N*,*N*-*bis*(1-ethyl-1*H*-benzimidazol-2-yl)-1*H*-benzimidazol-2-amine
bipy	2,2’-bipyridine
^{13}C	carbon-13
°C	degrees Celsius
Cy	cyclohexyl
d	doublet
dd	doublet of doublets
DAB	1,4-diaza-1,3-butadiene
Dipp	2,6-diisopropylphenyl
dt	doublet of triplets
δ(A)	chemical shift of nucleus A
DCM	dichloromethane
DMAP	4-dimethylaminopyridine
dmpm	1,1-*bis*(dimethylphosphino)methane
dppm	1,1-*bis*(diphenylphosphino)methane
dppom	1,1’-methylene-*bis*(1,1-diphenyl-phosphine oxide)
Et	ethyl
^{19}F	fluorine-19
g	grams
^{1}H	hydrogen
$\{^{1}H\}$	hydrogen decoupled
hr	hour(s)
HOMO	highest occupied molecular orbital
Hz	Hertz
^{i}Pr	*iso*-propyl
IR	infrared spectroscopy

K	Kelvin
LUMO	lowest unoccupied molecular orbital
m	medium intensity
m	multiplet
m.p.	melting point
Me	methyl
MeCN	acetonitrile
$^{n}J_{AB}$	*n*-bond coupling between nuclei A and B
mmol	millimole
NBD	norbornadiene
NBN	norbornene
NMR	nuclear magnetic resonance
OTf	trifluoromethanesulfonate (triflate)
^{31}P	phosphorus-31
PDI	2,6-pyridine(diimine)
Pico	4-picoline-*N*-oxide
Ph	phenyl
Phen	1,10-phenanthroline
ppm	parts per million
Pyr	pyridine
R	alkyl/aryl substituent
$r_{(cov)}$	covalent radius
$r_{(vdW)}$	van der Waals radius
Σ	sum of
σ	sigma bonds
s	strong intensity
s	singlet
T	temperature
t	triplet
tt	triplet of triplets
td	triplet of doublets

tdme	1,1,1-*tris*(diphenylphosphinomethyl)-ethane
Tpy	2,2’:6’,2”-terpyridine
Triphos	*bis*(2-diphenylphosphinoethyl)-phenylphosphine
TMS	trimethylsilyl
^{t}Bu	*tertiary*-butyl
$^{t}Bu_2$bipy	4,4’-di-*tert*-butyl-2,2’-dipyridyl
w	weak intensity
X	halide

"And in the end, the love you take is equal to the love you make."

—Paul McCartney, *The End*

Chapter 1. Introduction

1.1 General Introduction of Main Group Chemistry

Coordination chemistry of the transition metals has been explored for over 100 years, with early discoveries dating back to 1893 with Alfred Werner's structure proposal for ionic coordination compounds.[1] The continuous development of transition metal chemistry has pushed scientists to expand their exploration to the other groups of the periodic table, including the main group elements (groups 13 to 17) with group 15 representing the pnictogens. Early studies on the group 15 elements started with their development as donor molecules (ligands), with one example from 1988 showing how pnictogen complexes containing phosphorus or arsenic undergo substitution with carbon monoxide in a $M_3(CO)_{12}$ complex (M = Ru, Os).[2] Many research groups around the globe now specialize in the study and exploration of the chemistry of the main group elements, with the goal of deepening our understanding on how this group of interesting elements behave. Our goal in the Burford lab is to explore the reactivity of main group compounds, exhibiting new properties, leading to new precursors for the synthesis of new molecules, such as catalysts, polymers, and materials. One goal is the development of new main group complexes that may replace rare transition metals in catalysis, such as platinum and palladium, paving a new greener pathway to perform everyday chemistry.

1.2 Coordination Chemistry and Ligands

A coordination complex is a molecule which consists of a central acceptor atom or ion with other groups of atoms, such as neutral or ionic donor ligands, bonded to it. Coordination chemistry started with the exploration of the transition metals which has led to the development of the coordination chemistry of main group coordination complexes, where a main group element such as phosphorus, germanium, or tin is the central atom.[3] The centre of a complex is normally a Lewis acidic metal, meaning it is electron-poor, and is surrounded by one or more Lewis basic, electron-rich, ligands and/or substituents.

Typical donor molecules used in transition metal coordination chemistry are based on sp^2 nitrogen atoms such as 2,2'-bipyridine (bipy, **Scheme 1** (a)), which can exist on its own as a neutral compound, but also has a non-bonding pair of electrons available to donate to a metal centre. This feature is seen with other common nitrogen containing ligands such as 4,4'-di-*tert*-butyl-2,2'-bipyridine (^{t}Bu$_2$bipy), 4-dimethylaminopyridine (DMAP), and pyridine (Pyr) (**Scheme 1** (a-c) respectively). DMAP and Pyr are monodentate ligands, meaning they only bind through one site, while bipy and ^{t}Bu$_2$bipy are bidentate, binding through two sites.

Common non-nitrogen containing ligands used in coordination chemistry are phosphine ligands. Where phosphorus is a heavier pnictogen analogue of nitrogen, there are similarities in its behaviour. Phosphines are typical donors in interpnictogen coordination complexes[4], because they have a non-bonding lone pair readily available. A few examples of phosphine ligands are the monodentate triphenylphosphine, and the bidentate 1,2-*bis*(diphenylphosphino)ethane (**Scheme 1** (d) and (e)).

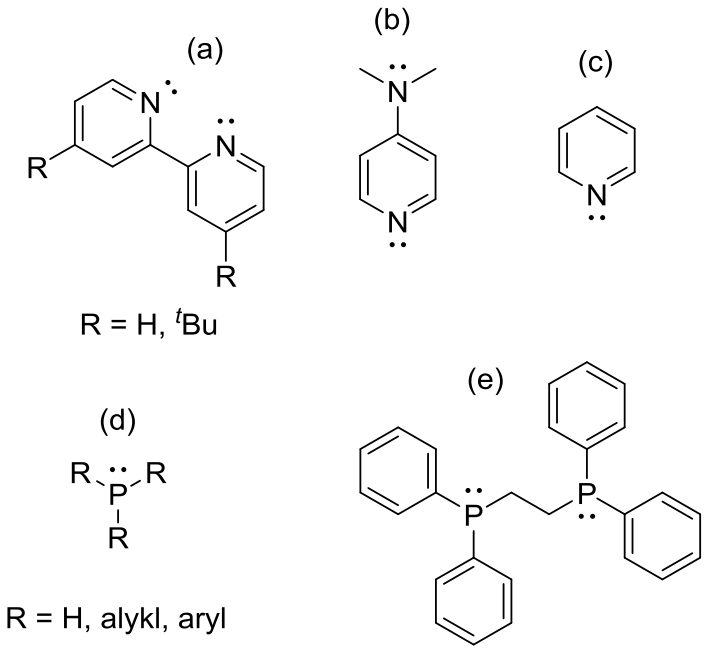

Scheme 1. Examples of common nitrogen and phosphorus containing ligands

Where phosphorus behaves primarily as a ligand, complexes featuring phosphorus as the Lewis acidic acceptor centre have not been thoroughly explored. However, by using the aforementioned 2,2'-bipyridine (where it has high basicity and oxidative resistance[5]) as the stabilizing ligandin this field of P(III) acceptor chemistry[6], a relationship between transition metal and main group coordination chemistry was achieved. By the early 2000s, it was proved that bipy can indeed donate to a P(III) centre (**Scheme 2**)[7,8], that these N-P(III) adducts can be formed, and that bipy can be used to stabilize P(III) centred complexes.[9]

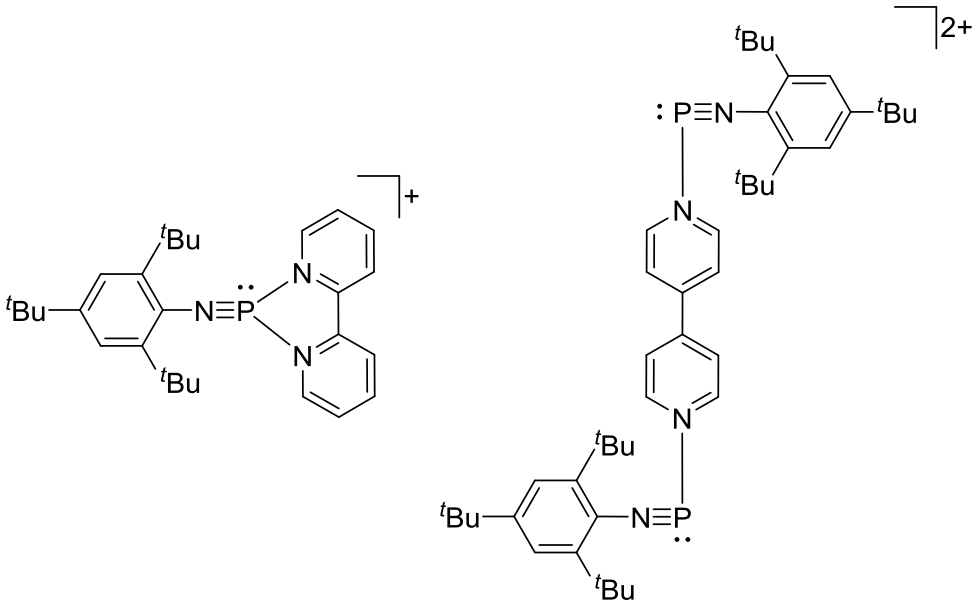

Scheme 2. 2,2’ and 4,4’ bipy ligands donating into P(III) complexes

1.3 Pnictogen Centred Cationic Complexes

A cation is a positively charged molecule or atom, meaning that the overall molecule/ion is missing one or more electrons. Examples of common polyatomic cations are shown in **Scheme 3**.

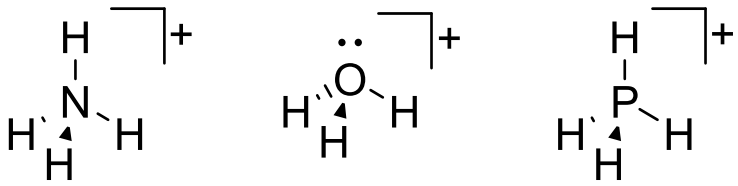

Scheme 3. Examples of isovalent polyatomic cations. From left to right: ammonium, hydronium, phosphonium

Cationic complexes can have interesting properties by being charged. For example, phosphine cations are more reactive and are likely to exhibit a higher Lewis acidity compared to their neutral counterparts, due to their lower LUMO energies[10]. There have been multiple examples of antimony and bismuth cationic centres, however smaller pnictogen centred

complexes (such as nitrogen or phosphorus centred) are rare.[11] Pnictogen centres are generally in the +3 or the +5 oxidation states[12], however Pn(III) centred complexes still have one non-bonding lone pair, increasing the electron density. This decreases the centre's ability to accept incoming donors, making them less Lewis acidic than traditional transition metals. However, the introduction of a cationic charge to the P(III) centre enhances its Lewis acidity, while still maintaining its lone pair of electrons.

The formation of the cation can be achieved through a one-pot synthesis where the halides of a PnX_3 (X = halide) compound can be abstracted and a donor ligand is introduced. **Scheme 4** shows that the Pn-X bond can be activated by reacting with silver trifluoromethanesulfonate (silver triflate; AgOTF), to generate a cation that may interact with a ligand. An equivalent of ligand is introduced and the formation of silver halide (AgX) pushes the reaction forward, forming the end tricationic product with three triflates acting as the counter ions.

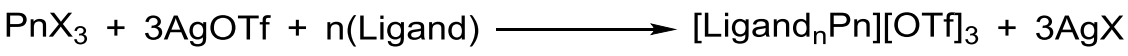

Scheme 4. General equation for the formation of a tricationic main group complex

The synthesis of dicationic phosphorus centred complexes can be achieved in the same way with the one-pot synthesis (**Scheme 5**) with TMSOTf as the halide abstractor instead of AgOTf.

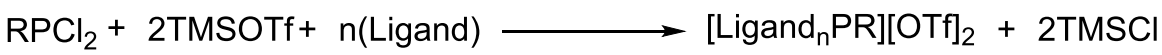

Scheme 5. General equation for the formation of a dicationic phosphorus centred complex

Triflate salts of phosphorus cationic complexes have been synthesised previously[7], but they have not been thoroughly explored. The complexes discussed in this thesis show the synthetic value of the Lewis acceptor behavior of $[P]^{3+}$ and $[PhP]^{2+}$ centres in the developing field of N-P(III) chemistry.[6] The now Lewis acidic P(III) central atom in the complex has an empty p-orbital available so that it can accept more donors, but still has its stereochemically active lone pair, making it ambiphilic. This introduces new reactivity pathways worthy of exploration where the Lewis acidic centre atom can also act as a donating centre. This enables a comprehensive study of the reactivity of the tricationic ($[P]^{3+}$) and dicationic ($[PhP]^{2+}$) complexes, containing bipy, $^{t}Bu_2$bipy, and other nitrogen and sulfur containing ligands. The formation of these main group coordination complexes will open doors to potential applications in catalysis, small molecule activation, or as precursors for polymers and materials (more discussed in **Chapter 2**.)

1.4 Recent Developments in Pn(III) Centred Cationic Complexes

The following describes the recent developments in the synthesis and isolation of interpnictogen cationic complexes of nitrogen, arsenic, antimony, and bismuth. This showcases the diversity of these compounds, and how their research is being developed. Phosphorus complexes will be discussed in the following chapters.

1.4.1 Nitrogen Centred Cationic Complexes

Similar to phosphorus, amines and imines behave primarily as Lewis donors; examples of nitrogen centres behaving as Lewis acceptors are rare, likely due to its small covalent radius and to the high Pauling electronegativity.[11] Nevertheless, nucleophilic displacement of R'_2NCl has resulted in the formation of $[R_3Pn\text{-}NR'_2][Cl]$ where Pn = N, P, and As (**Scheme 6**).[11,13–15]

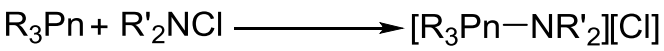

Scheme 6. Synthesis of $[R_3Pn\text{-}NR'_2][Cl]$ with Pn = N, P, and As; R = alkyl, aryl; R' = H, alkyl[11,13–15]

This small library of cationic nitrogen acceptors provides important parallels with heavier analogues of interpnictogen complexes.

1.4.2 Arsenic Centred Cationic Complexes

Arsenic centred cationic complexes are generally synthesised through N-As, P-As, and As-As donor-acceptor interactions, while examples of Sb-As, Bi-As complexes and ligand stabilized polycationic complexes of arsenic are rare.[11] The following are examples of the synthesis of various arsenic centred cationic complexes:

(1) S_N2 mechanism for the formation of a N-As complex.[11,16]

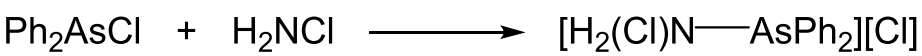

Scheme 7. Synthesis of $[H_2(Cl)N\text{-}AsPh_2][Cl]$[11,16]

(2) Nucleophilic displacement of a halide/OTf anion from arsine complexes using R_3P.[11,17]

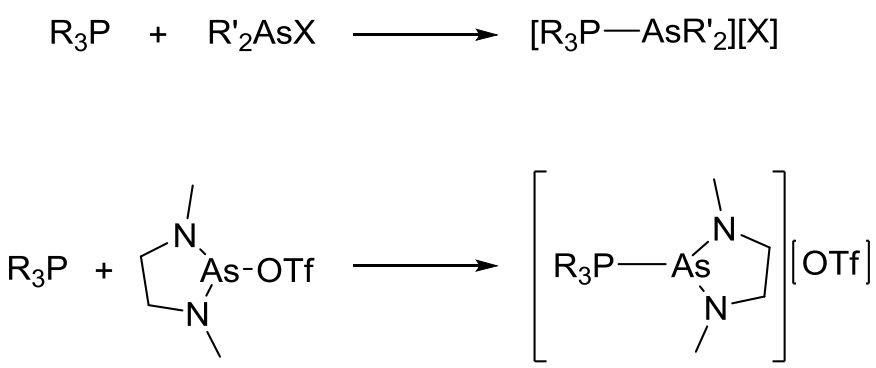

Scheme 8. Synthesis of $[R_3P\text{-}AsR'_2][X/OTf]$. R, R' = alkyl[11,17]

(3) The condensation of Me_2AsI with solid Ga_2I_4 was the first evidence for an arsenic cationic complex to form through homoatomic As-As coordination chemistry.[11,18]

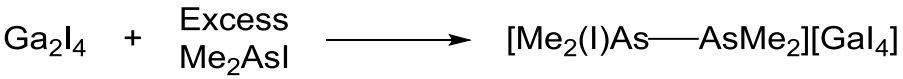

Scheme 9. Synthesis of $[Me_2(I)As\text{-}AsMe_2][GaI_4]$[11,18]

Arsenic centred interpnictogen cationic complexes continue to be explored, providing analogies with complexes of phosphorus, perhaps due to their similar covalent radii (P: 1.09 Å; As: 1.20 Å) and electronegativity (P: 2.19; As: 2.18)[19] (more in **Chapter 2**)

1.4.3 Antimony Centred Cationic Complexes

A wide array of Sb(III) acceptor complexes have been reported, due to the fact that the heavier *p*-block elements, while also having larger atomic radii, generally exhibit greater Lewis acidity than the lighter *p*-block elements.[11] However, as discussed earlier in this chapter, the Lewis

acidity of the Sb centre can still be enhanced by inducing a cationic charge through halide displacement/abstraction. The following are examples of mono-, di-, and tricationic antimony salts that have been recently reported.

Multidentate ligands have been used extensively in antimony centred complexes, including chelating phosphines such as 1,1-*bis*(diphenylphosphino)methane (dppm) and 1,1-*bis*(dimethylphosphino)methane (dmpm)[11,20] (**Scheme 10**) and chelating nitrogen containing ligands such as phenanthroline[11,21] (phen; **Scheme 11)** and bipy[5,11] (**Scheme 12)**. While the heavier pnictogen centred complexes have a larger coordination sphere, they can accommodate chelating ligands better than their lighter pnictogen analogues.

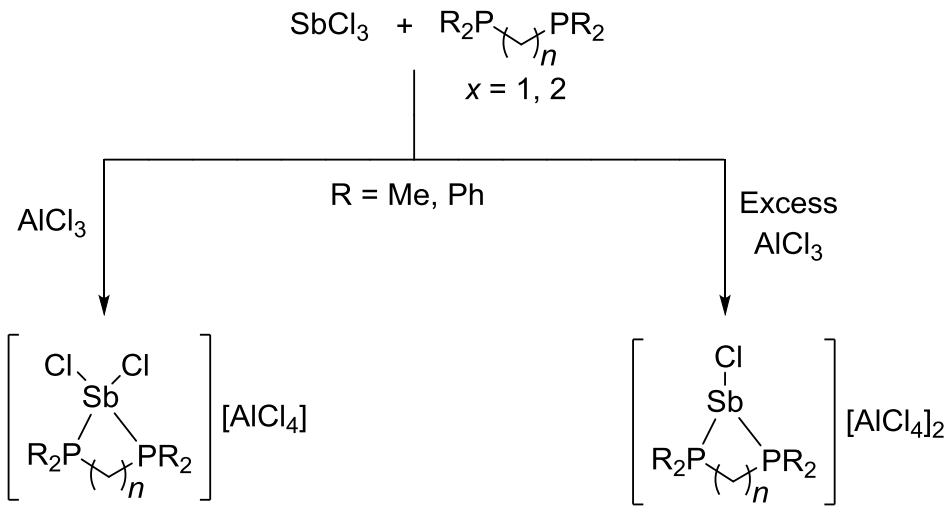

Scheme 10. Synthesis of complexes of $SbCl_2^+$ and $SbCl^{2+}$ with chelating diphosphines[11,20]

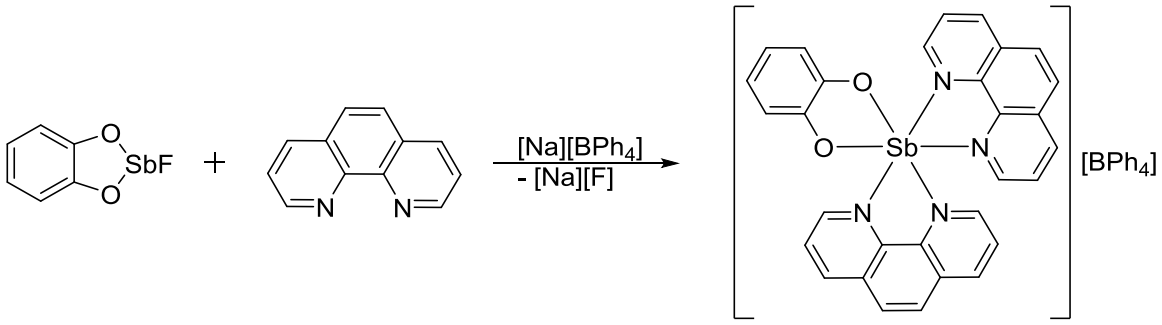

Scheme 11. Intermolecular N-Sb coordinate bonding *via* synthesis of $[(phen)_2Sb(O_2C_6H_4)][BPh_4]$[11,21]

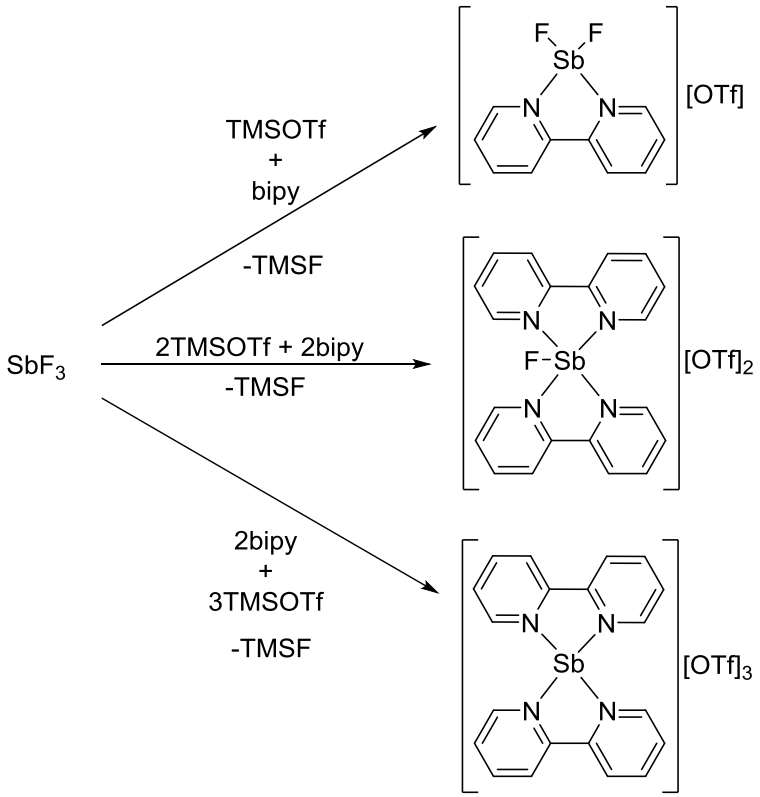

Scheme 12. 2,2'-bipyridine complexes of $[SbF_{3-x}]^{x+}$ synthesis [5,11]

Monodentate ligands have also been used in these complexes: for example, Ph_3P[11,22] (**Scheme 13**) and R_3As (R = Me, Ph)[11,23] (**Scheme 14**).

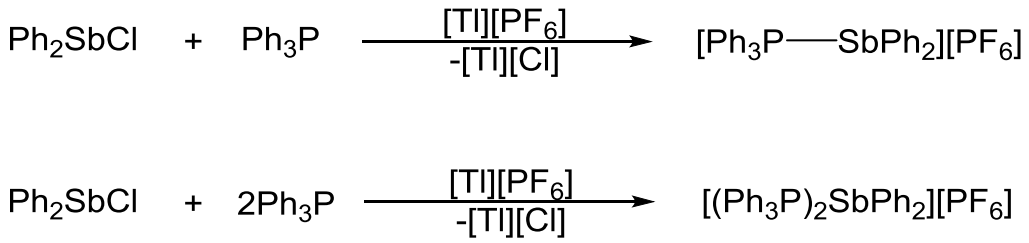

Scheme 13. Synthesis of $[Ph_3P\text{-}SbPh_2][PF_6]$ (top) and $[(Ph_3P)_2SbPh_2][PF_6]$ (bottom)[11,22]

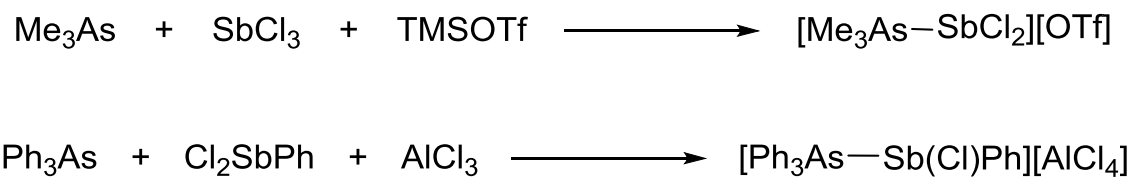

Scheme 14. Synthesis of $[R_3As\text{-}Sb(Cl)R'][X]$ salts[11,23]

1.4.4 Bismuth Centred Cationic Complexes

Despite having a higher Lewis acidity like Sb, as described in section **1.4.3**, bismuth centred cationic complexes are the least developed of interpnictogen cationic complexes.[11] While there are numerous reports of bismuthenium cationic complexes stabilized by Group 16 donors (such as $OPPh_3$[24] and $OP(NMe_2)_3$[11,24–27]), there are only a few examples of interpnictogen stabilized bismuthenium cationic complexes; mostly with chelating ligands.[11] As mentioned previously, this is most likely due to the fact that bismuth has a much larger coordination sphere and is more likely to interact with several multidentate ligands.[11]

Similar to antimony centred cationic complexes, reactions of bismuth containing compounds with Ph_3P (**Scheme 15**)[11,22], Ph_3As (**Scheme 16**)[11,23,28], and a variety of pyridyl ligands (**Scheme 17**)[11,24,29] have been reported. Reactions of $BiCl_3$ with Ph_3Sb have also been reported (**Scheme 18**).[11,28]

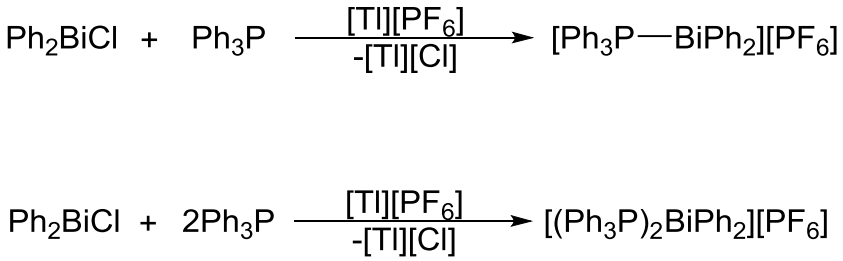

Scheme 15. Synthesis of $[Ph_3P\text{-}BiPh_2][PF_6]$ (top) and $[(Ph_3P)_2\text{-}BiPh_2][PF_6]$ (bottom)[11,22]

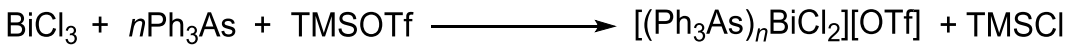

Scheme 16. Synthesis of $[(Ph_3As)_nBiCl_2][OTf]$ (n = 1 or 2) salts[11,23,28]

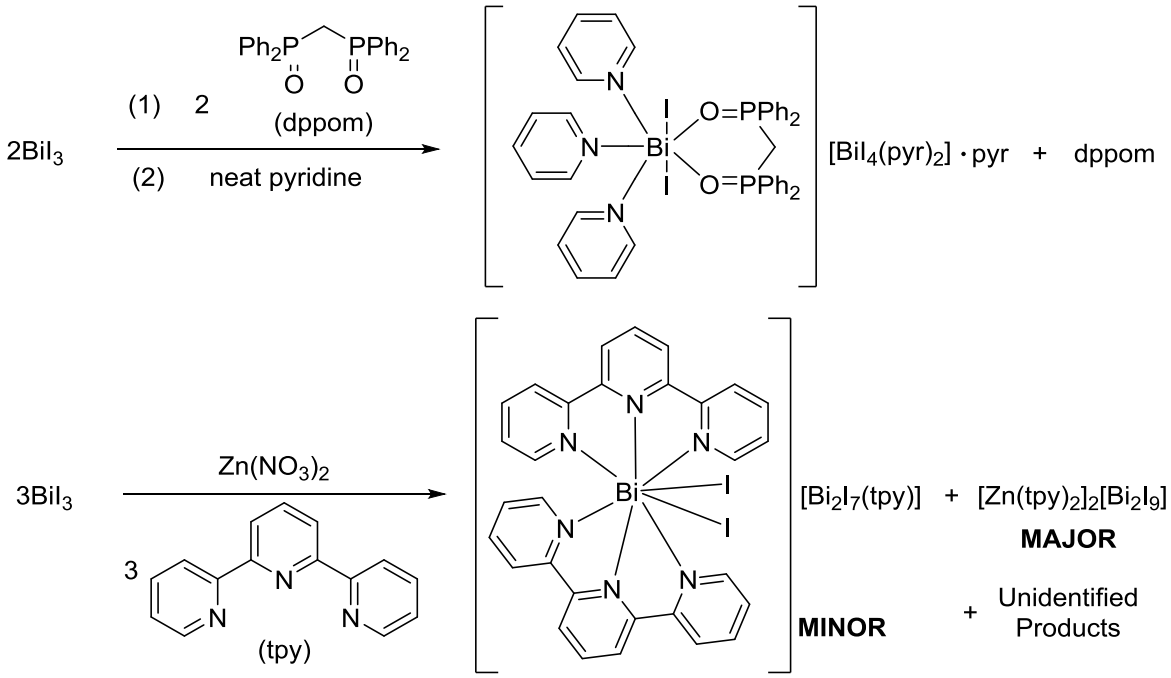

Scheme 17. Synthesis of $[BiI_2(pyr)_3(dppom)][BiI_2(pyr)_2]\cdot pyr$ (top) and $[BiI_2(tpy)_2][Bi_2I_7(tpy)]$[11,24,29]

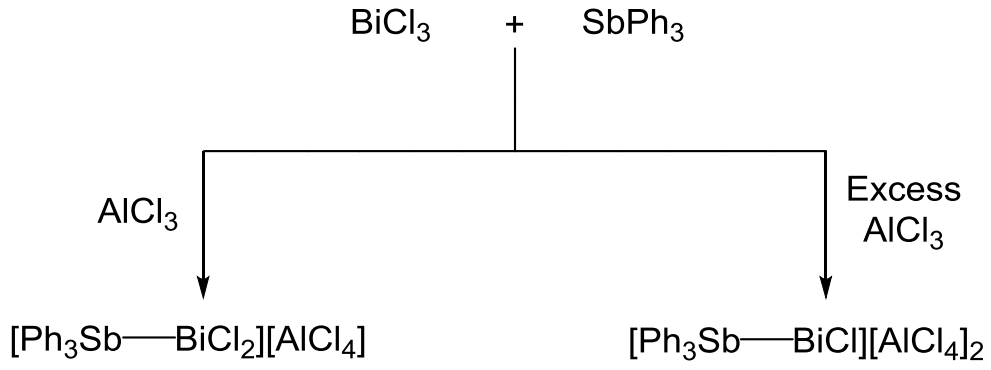

Scheme 18. Synthesis of $[(Ph_3Sb\text{-}BiCl_2][AlCl_4]$ (left) and $[(Ph_3Sb\text{-}BiCl][AlCl_4]_2$ (right)[11,28]

Chapter 2. P(III) Centred Tricationic Complexes

2.1 Introduction

Prior to 2010, only three examples of P(III) tricationic complexes were reported, but were not structurally characterized (the connectivity of the atoms in the formed species was determined based on spectroscopic methods and melting points). Those three examples are reported to be stabilized by the nitrogen based ligands: DMAP[30], quinuclidine[30], and 1,5-diazabicyclo[4.3.0]non-5-ene[31], with three triflate counter anions (**Scheme 19**).

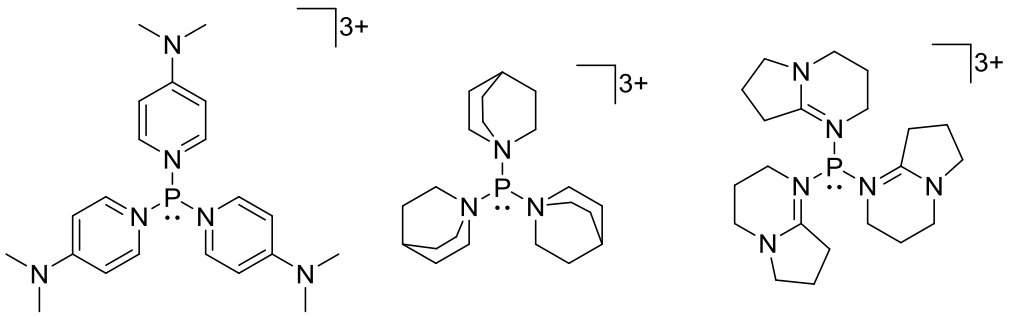

Scheme 19. Proposed structures of N-stabilized $[P]^{3+}$ complexes using DMAP[30], quinuclidine[30], and 1,5-diazabicyclo[4.3.0]non-5-ene[31]

It was only in 2010 that the first structurally characterized examples of a P(III) tricationic complex were reported. These complexes were Janus head type complexes, stabilized by nitrogen containing ligands: the diphosphorus tricationic complex[32] and the single phosphorus tricationic complex (**Scheme 20**).[33]

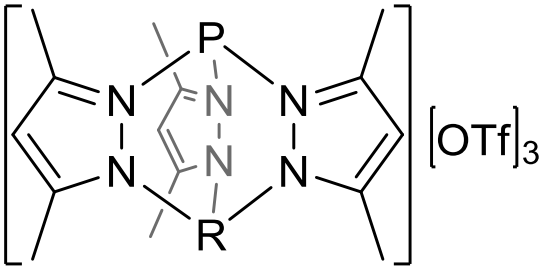

Scheme 20. Janus head type $[P]^{3+}$ complexes, where R = P[32] or R = C-H[33]

These nitrogen containing ligands have high stability and oxidative resistance, similar to that of carbene ligands. Because of their outstanding donor properties, carbene ligands were used to stabilize these Lewis acidic centres. This was achieved by the reaction of three equivalents of a 1-chloro-2,3-*bis*(dialkylamino)cyclopropenium salt with $P(SiMe_3)_3$ (**Scheme 21**) to yield a carbene-stabilized $[P]^{3+}$ complex.[34]

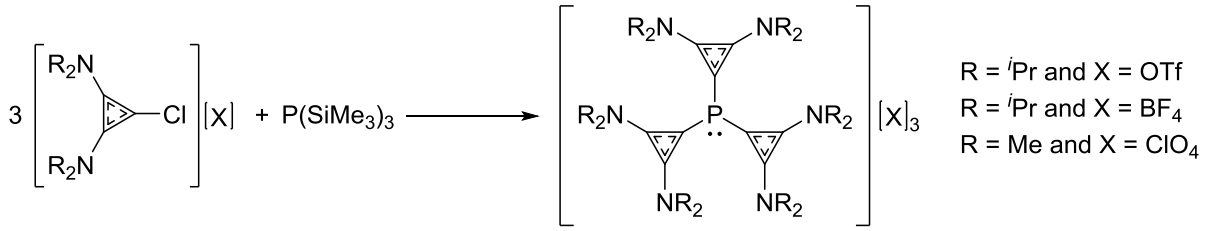

Scheme 21. Synthesis of carbene-stabilized $[P]^{3+}$ complexes[34]

The use of oxidatively resistant donors in these complexes have prompted the development of a series of nitrogen stabilized tricationic *tris*-triflate salts using phosphorus, arsenic, antimony, and bismuth, which have been successfully synthesised and characterized (**Scheme 22**).[35]

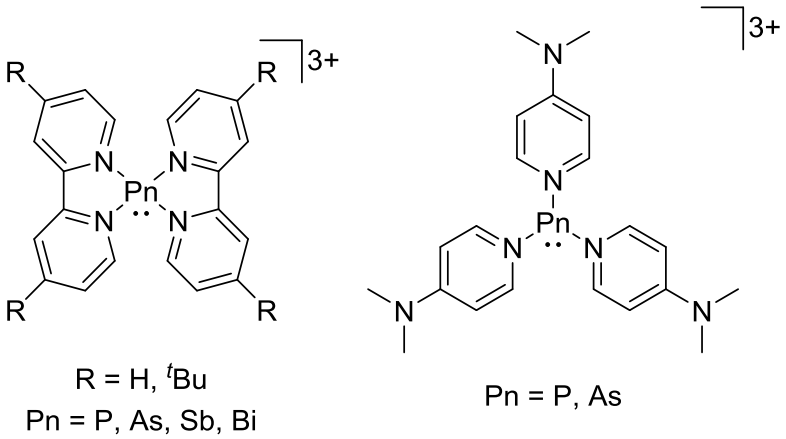

Scheme 22. General Lewis structures of previously synthesised Pn tricationic complexes

Solid-state structures of $[Pn(bipy)_2][OTf]_3$ where Pn = P, Sb, and Bi, $[Pn\ (^tBu_2bipy)_2][OTf]_3$ where Pn = P, As, and Sb, and $[Pn\ (DMAP)_3][OTf]_3$ where Pn = P and As, were determined by X-ray crystallography. The successful isolation of the $[As(bipy)_2][OTf]_3$ and $[Bi(^tBu_2bipy)_2][OTf]_3$ complexes have been confirmed by NMR spectroscopy, but a crystal structure has not yet been obtained.[35]

Since these complexes have high Lewis acidity and a non-bonding lone pair available to donate, their reactivity is of high interest where they can be envisaged to activate small molecules[3] (more later). However, only preliminary studies of these Pn^{3+} complexes have been explored. The most Lewis acidic Pn^{3+} complex is where Pn = P, based on charge density calculations and ligand dissociation energies in the gas phase (the trend being Pn = Bi < Sb < As < P).[35] Because of this, the non-bonding lone pair is expected to be the least reactive of the series, allowing the acceptor ability of the Lewis acidic centre of the complex to be primarily studied. Trends built on the research of the phosphorus complexes are speculated to be paralleled by the heavier analogues. The phosphorus complexes can also be easily monitored using $^{31}P\{^1H\}$ NMR spectroscopy.

The exploration of $[P(^tBu_2bipy)_2][OTf]_3$ has been selected over $[P(bipy)_2][OTf]_3$ and $[P(DMAP)_3][OTf]_3$ simply because the former is more soluble and the ^{t}Bu groups are easily identifiable by NMR spectroscopy.

Reactions of $[P(^tBu_2bipy)_2][OTf]_3$ (**[1]$^{3+}$**; **Scheme 23**) were attempted with a diverse selection of compounds in order to assess its reactivity and have already revealed a number of new reactivity patterns. The absence of the starting material **[1]$^{3+}$** chemical shift ($\delta = 30.6$ ppm) in the $^{31}P\{^1H\}$ NMR spectrum, and the presence of any new chemical shift(s) indicates the formation of a new compound. Therefore, reactions will be described using their spectra, and solid-state structures will be discussed when applicable. The successful reactions will be discussed in detail, however a full list of all performed reactions can be found in **Tables 1-7**. Please note that for clarity, the $^tBu_2bipy$ ligands will be denoted as shown (**Scheme 23**) in the reaction schemes.

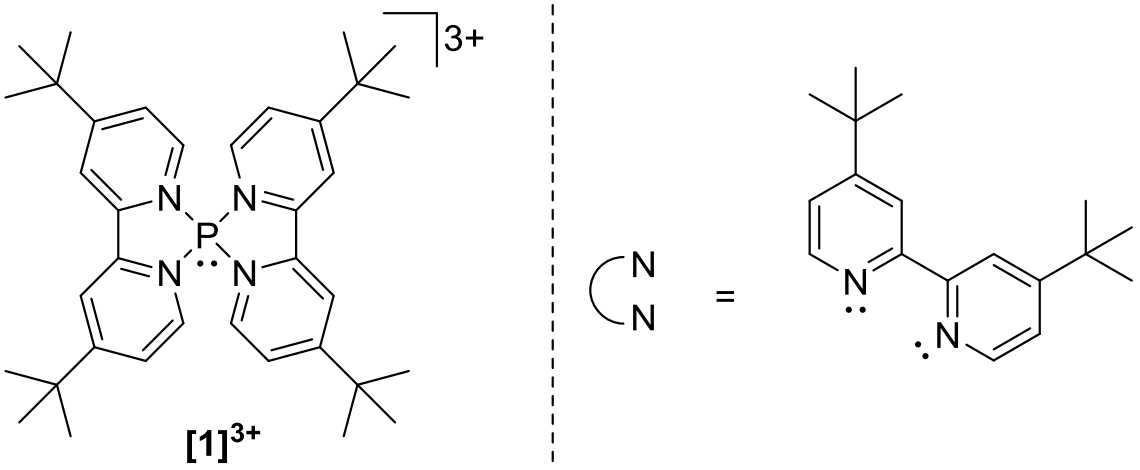

Scheme 23. Compound **[1]$^{3+}$**; representation of $^tBu_2bipy$ in the following schemes

As a starting point for the development of the reactivity of **[1]$^{3+}$**, preliminary studies involving the potential activation of C-H and H-H bonds were attempted previously in the Burford Group. 1:2 combinations of **[1]$^{3+}$** with $^tBu_3P$ in CD_3CN dehydrogenate 1,4-cyclohexadiene to form benzene, $[^tBu_3P\text{-}H]^+$ as seen in the ^{31}P NMR spectrum, and a mixture of other unidentified products, none of which contain $^1J_{PH}$ coupling. ^1H and $^{31}P\{^1H\}$ NMR analysis show the complete consumption of the starting materials and the formation of the new products, providing evidence for the potential activation of the C-H bond in cyclohexadiene (top in **Scheme 24**)[35].

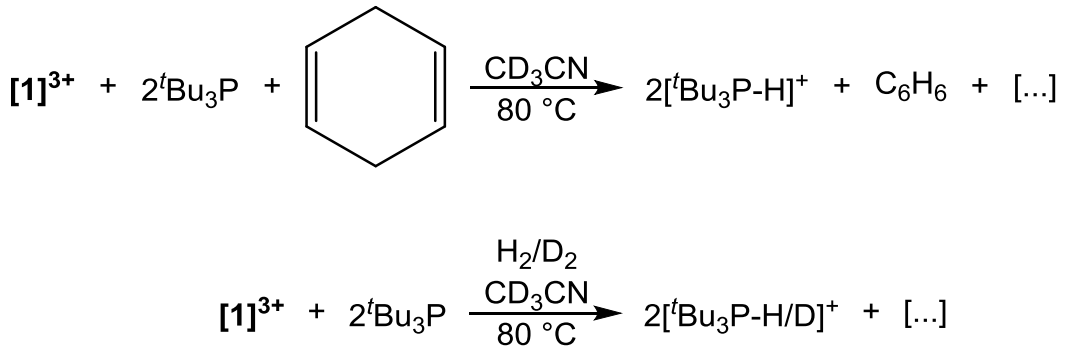

Scheme 24. C-H and H-H bond activation by **[1]$^{3+}$**. Adapted from Reference 35[35]

The same 1:2 mixture with H_2 or D_2 (1 atm pressure) also resulted in the complete conversion of $^{t}Bu_3P$ to $[^{t}Bu_3P\text{-}H]^+$ or $[^{t}Bu_3P\text{-}D]^+$ by ^{31}P NMR spectroscopy, along with other unidentifiable products (bottom in **Scheme 24**). These reactions need to be explored further, but the preliminary results provide evidence for the possible activation of C-H and H-H bonds, and showcase the potential of **[1]$^{3+}$** as a viable compound for the activation of other small molecules such as CO_2, CO, N_2, and NO.

In all cases in this thesis, the magnitude of the positive charge on all complexes are balanced by an equivalent number of OTf anions. Specific reactions will be described using the code [Table #]-[entry #], for example, 1-1 refers to Table 1 first row. Full reaction conditions can be found at the end of each section in their corresponding table (**Tables 1 – 7**).

2.2 $[1]^{3+}$ Acting as an Electrophile

The electrophilic reactivity of $[1]^{3+}$ was assessed (**Table 1**). Reactions with Ph_3PO (**1-3**/**1-4**) and Cy_3PS (**1-9**) were attempted (**Scheme 25**). An equimolar reaction was performed in MeCN, stirred for at least 1 hr, and then monitored by $^{31}P\{^1H\}$ NMR spectroscopy. The resulting product was washed with diethyl ether three times and the final material was assessed by heteronuclear NMR spectroscopy.

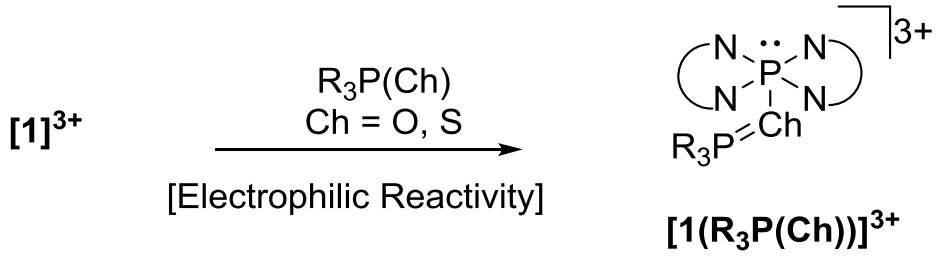

Scheme 25. Proposed reaction and structure for electrophilic reactivity assessment

Reaction **1-3** was performed in MeCN and reaction **1-4** was performed in DCM to see if solvent had any effect on the reaction. Although the starting material is only partially soluble in DCM, a reaction was observed by NMR spectroscopy. In the $^{31}P\{^1H\}$ NMR spectrum for **1-3**, two major chemical shifts at 37.1 ppm and 29.9 ppm were observed, and in **1-4**, similar shifts at 33.4 ppm and 29.6 ppm were observed. This is interpreted to be the result of the formation of an adduct in solution, as seen in the more deshielded shift of the donor Ph_3PO from 23.2 ppm[36] to 37.1 ppm or 33.4 ppm respectively, and the more shielded shift of the acceptor $[1]^{3+}$ from 30.6 ppm to 29.9 or 29.6 respectively. This however cannot be confirmed without evidence from 2D NMR experiments. Unfortunately, attempts to crystallize the product lead to the isolation of starting material or the protonated ^{t}Bu$_2$bipy ligand. This has been seen frequently while performing these reactions. This is likely due to the ligand becoming more basic in the presences of the cation, and while MeCN is coordinating to the centre, the C-H bond in the solvent activates, making the ligand react with the more protic hydrogen, forming ^{t}Bu$_2$bipy-H$^+$.

Table 1. Reactions of $[1]^{3+}$ Acting as an Electrophile with Various Reagents

Entry	Reagent	Solvent	Heated temp. (°C); time (hr)	$^{31}P\{^{1}H\}$ NMR δ (ppm)	Assignment
1	Ph_2S_2	MeCN	70; 4	30.6	$\mathbf{[1]^{3+}}$
2	Diphenylbutadiene	MeCN	75; 16	136.7	$\mathbf{[1(Ph_2C_4H_4)]^{3+}}$
3	Ph_3PO	MeCN	-	37.1	$\mathbf{[1(Ph_3PO)]^{3+}}$
4	Ph_3PO	DCM	-	33.4, 29.6	$\mathbf{[1(Ph_3PO)]^{3+}}$
5	Ph_3PO	DCM	-	30.6	$\mathbf{[1]^{3+}}$
6	Ph_3PO	DCM	-	26.9	$\mathbf{[1(Ph_3PO)]^{3+}}$
7	$2(Ph_3PO)$	DCM	-	27.5	$\mathbf{[1(Ph_3PO)]^{3+}}$
8	Et_3PO	MeCN	-	-	-
9	Cy_3PS	MeCN	-	118.6	-

Reactions were performed at room temperature and were stirred for 1 hr and then assessed by $^{31}P\{^{1}H\}$ NMR spectroscopy. Mixtures were stirred overnight if starting material was still present in the $^{31}P\{^{1}H\}$ NMR spectrum. Mixtures were then heated if starting material was still present in the $^{31}P\{^{1}H\}$ NMR spectrum. Assignments of $\mathbf{[1]^{3+}}$ indicate no reaction. Assignments of – indicate that the resulting compound cannot be determined/peak(s) cannot be assigned.

2.3 $[1]^{3+}$ Acting as a Nucleophile

The nucleophilic reactivity of $[1]^{3+}$ was assessed by the reaction with MeOTf (**2-2**) (**Scheme 26**) and diphenylacetylene (**Table 2**). For the reaction of $[1]^{3+}$ with MeOTf, equimolar amounts were combined in MeCN, stirred for 15 mins, and then assessed by $^{31}P\{^{1}H\}$ NMR spectroscopy. The major chemical shift in the spectrum was assigned to the starting material $[1]^{3+}$ at 30.6 ppm, with a minor shift at 109.9 ppm. The mixture was left to stir for another 2 hr, where a colourless slurry formed. The slurry was analyzed by $^{31}P\{^{1}H\}$ NMR spectroscopy, showing four singlets not present in the starting material spectrum, δ = 100 ppm: 110.1 ppm, 129.0 ppm, 132.3 ppm, and 140.2 ppm, with similar intensities, with no starting material peak present. This is consistent with an increase in positive charge to +4, where the lone pair is now donating to the Me group, decreasing the electron density at the P centre, producing a more deshielded chemical shift.

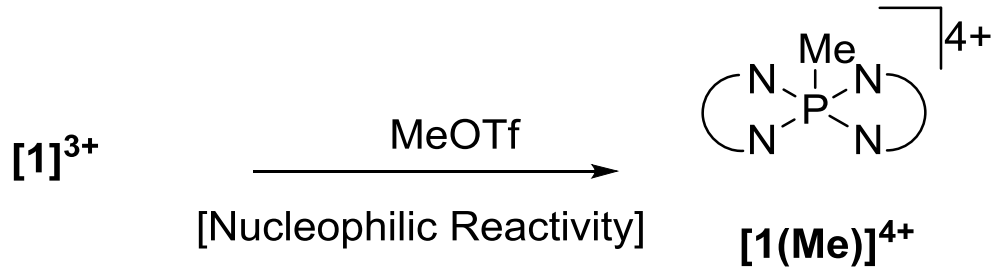

Scheme 26. Proposed reaction and structure for nucleophilic reactivity assessment

The product was assessed by ^{31}P NMR spectroscopy to see if there were any coupling with a hydrogen atom from a CH_3 group, but unfortunately, no coupling was observed. With more than one phosphorus chemical shift present in the $^{31}P\{^{1}H\}$ NMR spectrum, it is challenging to deduce a proposed structure, although ^{1}H NMR spectroscopy shows the presence of methylated ligand, [($^{t}Bu_2$bipy)Me][OTf].

Table 2. Reactions of $[1]^{3+}$ Acting as a Nucleophile with Various Reagents

Entry	Reagent	Solvent	Heated temp. (°C); time (hr)	$^{31}P\{^{1}H\}$ NMR δ (ppm)	Assignment
1	PhC≡CPh	MeCN	70; 4	30.6	$\mathbf{[1]^{3+}}$
2	MeOTf	MeCN	-	109.9	-
3	MeOTf	MeCN	-	110.1	-

Reactions were performed at room temperature and were stirred for 1 hr and then assessed by $^{31}P\{^{1}H\}$ NMR spectroscopy. Mixtures were stirred overnight if starting material was still present in the $^{31}P\{^{1}H\}$ NMR spectrum. Mixtures were then heated if starting material was still present in the $^{31}P\{^{1}H\}$ NMR spectrum. Assignments of $\mathbf{[1]^{3+}}$ indicate no reaction. Assignments of – indicate that the resulting compound cannot be determined/peak(s) cannot be assigned.

2.4 Reactions of $[1]^{3+}$ with Bicyclo reagents by Oxidative Addition

Where $[1]^{3+}$ has already been shown to activate H_2 and 1,4-cyclohexadiene as discussed in section **2.1**, $[1]^{3+}$ was combined with norbornene (NBN), with norbornadiene (NBD) (**Scheme 27**), and with cyclohexene, in attempts to perform an oxidative addition (1,2-cycloaddition fashion) (**Table 3**). Equimolar amounts were combined in MeCN, forming a clear yellow solution. Samples were analyzed every few hours by $^{31}P\{^{1}H\}$ NMR spectroscopy, but no change in the spectra was observed. Both reactions were heated in a thick walled cylindrical glass tube with a Teflon screwcap, called a reaction bomb, at 75 °C for 16 hr.

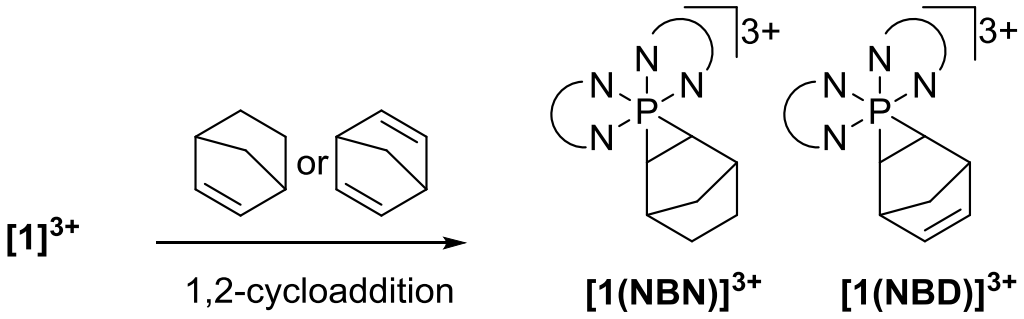

Scheme 27. Proposed reaction and structure for the 1,2-cycloaddition with NBN or NBD

After analysing the NBN (**3-2**) reaction with $^{31}P\{^{1}H\}$ NMR spectroscopy, the major peak was assigned to $[1]^{3+}$, although a few other insignificant peaks were observed. Two more equivalents of NBN were added and the reaction was heated again for 16 hr at 75 °C. The resulting red-orange solution was assessed by $^{31}P\{^{1}H\}$ NMR spectroscopy, and the resulting spectrum contained a major singlet peak at δ = 138.9 ppm and two minor singlet resonances at δ = 84.5 ppm. A brown-red solid was isolated, however, recrystallization from MeCN only resulted in the isolation of long colourless needles, which have been assigned to protonated $^{t}Bu_2$bipy ligand.

Several new chemical shifts in the $^{31}P\{^{1}H\}$ NMR spectrum were observed with the reaction of $[1]^{3+}$ with NBD (**3-3**) after the solution was heated for 16 hr at 75 °C. Two singlet resonances at δ = 79.6 ppm and 138.9 ppm with similar intensities were observed. The peak at

138.9 ppm matches the chemical shift observed in the NBN reaction. From this, it can be speculated that both reactions, **3-2** and **3-3**, produce the same product, however, there is no literature evidence to support the tricationic predicted species. A deshielded shift of 138.9 ppm could potentially be the formation of a phosphorus centred dicationic complex, where they have chemical shifts in this region. More information is needed to fully identify the complex. The brown-red isolated solid was recrystallized from MeCN, but unfortunately the resulting colourless crystals have been assigned to protonated $^{t}Bu_2$bipy ligand.

Where the formation of protonated ligand has been an issue when using MeCN as the solvent, the reactions were repeated in toluene and DCM, but no reaction took place in either situation (only starting material observed in the $^{31}P\{^{1}H\}$ NMR spectrum) and DCM cannot be extensively heated (max 40 °C) to facilitate the reaction.

Table 3. Reactions of $[1]^{3+}$ with Ring Compounds by Oxidative Addition

Entry	Reagent	Solvent	Heated temp. (°C); time (hr)	$^{31}P\{^{1}H\}$ NMR δ (ppm)	Assignment
1	Cyclohexene	MeCN	70; 4	30.6	$[1]^{3+}$
2	3NBN	MeCN	70; 48	138.9	-
3	NBD	MeCN	75; 16	138.9	-
4	3NBN	DCM	45; 16	-	-
5	3NBN	Toluene	75; 16	30.6	$[1]^{3+}$

Reactions were performed at room temperature and were stirred for 1 hr and then assessed by $^{31}P\{^{1}H\}$ NMR spectroscopy. Mixtures were stirred overnight if starting material was still present in the $^{31}P\{^{1}H\}$ NMR spectrum. Mixtures were then heated if starting material was still present in the $^{31}P\{^{1}H\}$ NMR spectrum. Assignments of $[1]^{3+}$ indicate no reaction. Assignments of – indicate that the resulting compound cannot be determined/peak cannot be assigned.

2.5 Oxidation of $[1]^{3+}$

A series of reactions were carried out to see if $[1]^{3+}$ would oxidize in the presence of various halogen sources (**Table 4**). It has been reported previously that $[1]^{3+}$ reacts cleanly with sulfuryl chloride, SO_2Cl_2, to form the oxidized complex $[1(Cl_2)]^{3+}$ (**Scheme 28**), as evidence by a single peak in the $^{31}P\{^1H\}$ NMR) spectrum at δ = -146.9 ppm.[35]

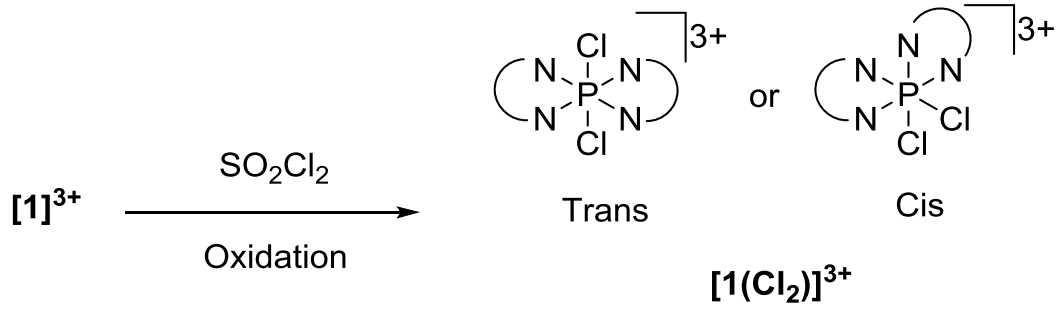

Scheme 28. Oxidation of $[1]^{3+}$ with SO_2Cl_2

To test whether a similar product can be obtained with other halides, $[1]^{3+}$ was reacted with I_2 and Br_2. An equimolar mixture of $[1]^{3+}$ and I_2 were heated at 75 °C for 16 hr (**4-2**) in a reaction bomb, $^{31}P\{^1H\}$ NMR spectroscopic measurements of the resulting mixture only yielded the starting material chemical shift at 30.6 ppm. From this it can be concluded $[1]^{3+}$ does not react with I_2.

When reacted with one equivalent of Br_2 (**4-6**), the only peak observed by $^{31}P\{^1H\}$ NMR spectroscopy was obtained at δ = -5.9 ppm. This is very similar to the product observed if one equivalent of H_2O is added to $[1]^{3+}$ in MeCN, which has been reported to be a mixture of protonated ^{t}Bu$_2$bipy and H_3PO_3 by ^1H and $^{31}P\{^1H\}$ NMR spectroscopy.[37]

As a side note, when reacted with 4-picoline-*N*-oxide (pico) (**4-3**), it was hypothesised that $[1]^{3+}$ would undergo some electrophilic reactivity (top in **Scheme 29**). However, the $^{31}P\{^1H\}$ NMR) spectrum showed a single chemical shift at -112.1 ppm. Since the oxidation of $[1]^{3+}$ with SO_2Cl_2 yielded a peak at δ = -146.9 ppm, and reported P(V) complexes have similar

reported shifts ($[(DMAP)_2PCl_4]^+$ δ = -196 ppm[38] and $[(bipy)PCl4]^+$ δ = -191 ppm)[39], the proposed structure was reassessed and it is now hypothesised that the resulting compound may be an oxidation product (bottom in **Scheme 29**).

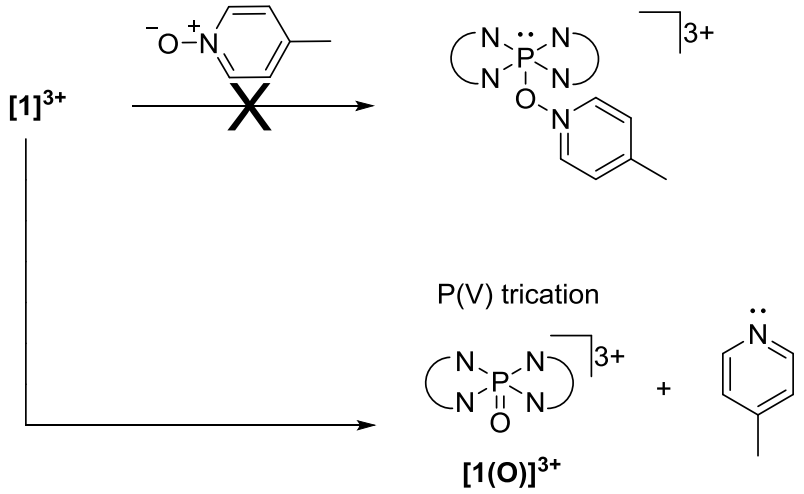

Scheme 29. First proposed structure (top) and reassessed oxidation structure (bottom)

The isolated dark brown solid was recrystallized from MeCN; however, the resulting colourless crystals were assigned to the protonated $^tBu_2$bipy ligand.

Table 4. Oxidation of $[1]^{3+}$ with Various Reagents

Entry	Reagent	Solvent	Heated temp. (°C); time (hr)	$^{31}P\{^{1}H\}$ NMR δ (ppm)	Assignment
1	SO_2Cl_2	MeCN	-	-146.9	$\mathbf{[1(Cl_2)]^{3+}}$
2	I_2	MeCN	70; 4	30.6	$\mathbf{[1]^{3+}}$
3	Pico	MeCN	-	-112.1	$\mathbf{[1(O)]^{3+}}$
4	Excess S_8	MeCN	75; 16	30.6	$\mathbf{[1]^{3+}}$
5	H_2O	MeCN	-	-5.9	$\mathbf{H_3PO_3}$
6	Br_2	MeCN	-	-5.9	$\mathbf{H_3PO_3}$

Reactions were performed at room temperature and were stirred for 1 hr and then assessed by $^{31}P\{^{1}H\}$ NMR spectroscopy. Mixtures were stirred overnight if starting material was still present in the $^{31}P\{^{1}H\}$ NMR spectrum. Mixtures were then heated if starting material was still present in the $^{31}P\{^{1}H\}$ NMR spectrum. Assignments of $\mathbf{[1]^{3+}}$ indicate no reaction.

2.6 Reduction of $[1]^{3+}$

$[1]^{3+}$ was reacted with various reagents to see if it could be reduced (**Table 5**). Three equivalents of $[1]^{3+}$ were reacted with two equivalents of Mg powder (**5-1**) or Zn powder (**5-4**), with the idea being that three equivalents of $[1]^{3+}$ would act as a 9+ complex, $3[1]^{3+}$, and reduce to a 5+ complex, $[2]^{5+}$ (**Scheme 30**).

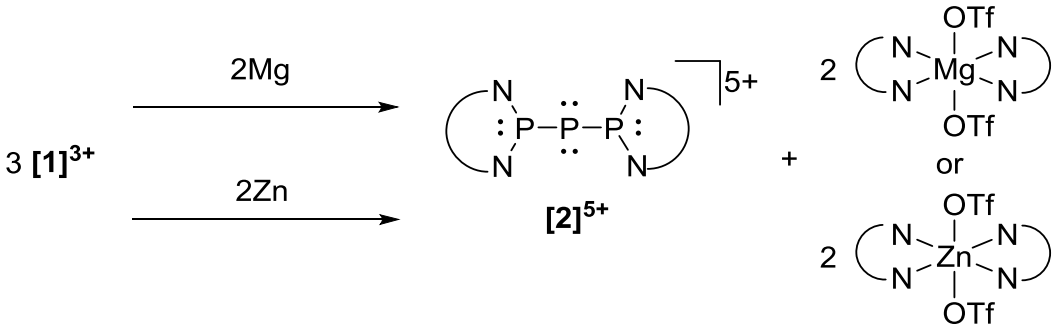

Scheme 30. Proposed formation of $[2]^{5+}$ by a two-electron reduction of $[1]^{3+}$ with Zn or Mg

When combined with Mg and left to stir for a few hours, the resulting $^{31}P\{^{1}H\}$ NMR spectrum showed a triplet at δ = 84.9 ppm and a doublet at 238.3 ppm (**Figure 1**). This corresponds with the proposed structure $[2]^{5+}$, where the two terminal phosphorus atoms that are equivalent are split by the centre phosphorus atom and vice versa. However, attempts to crystallize the compound resulted in the isolation of the octahedral Mg salt by-product (**Figure 2**).

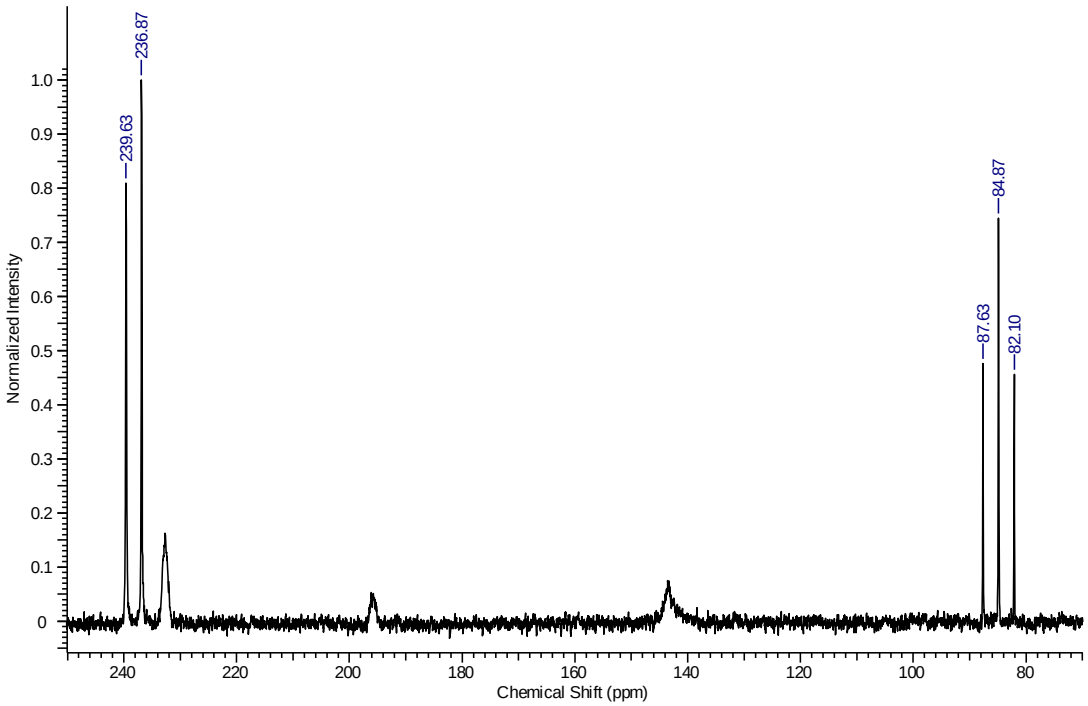

Figure 1. $^{31}P\{^{1}H\}$ NMR) spectrum of **[2]**$^{5+}$ and a few impurities

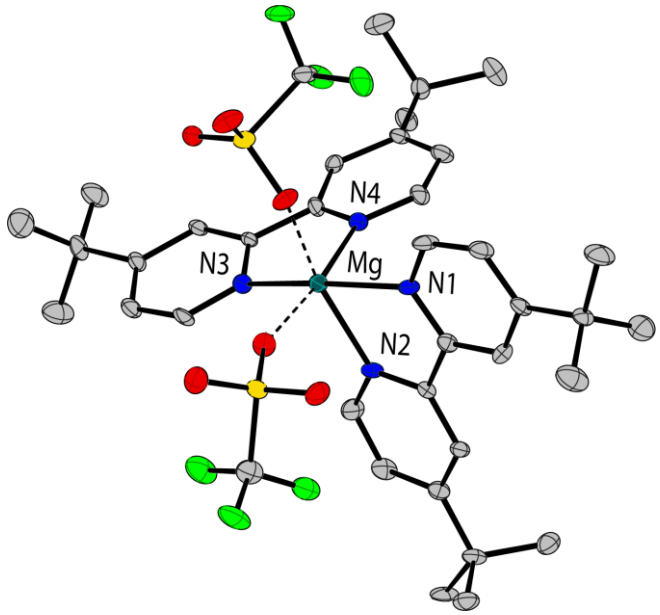

Figure 2. Solid-state structure of the Mg salt by-product $[Mg(^{t}Bu_2bipy)_2][OTf]_2$ in the reduction of **[1]**$^{3+}$

Thermal ellipsoids are shown at a 50% probability level. For clarity, hydrogen atoms and solvents are omitted. The interaction between the magnesium centre and all other atoms are outside the sum of the O-Mg covalent radii ($\Sigma_{r,cov}$(O, Mg) = 2.02 Å)[40] and the N-Mg covalent radii($\Sigma_{r,cov}$(N, Mg) = 2.10 Å)[40], but inside the sum of the O-Mg van der Waals radii ($\Sigma_{r,vdW}$(O, Mg) = 4.01 Å)[41] and of the N-Mg van der Waals radii ($\Sigma_{r,vdW}$(N,Mg) = 4.16 Å).[41]

When **[1]**$^{3+}$ was combined with Zn and left to stir for 3 days, the resulting $^{31}P\{^{1}H\}$ NMR spectrum showed no starting material chemical shift and a single peak at δ = 133.3 ppm. This contradicts the hypothesised structure **[2]**$^{5+}$, where it was predicted to have two phosphorus environments, and have multiple splitting patterns. The isolated pale-yellow powder was recrystallized from MeCN and the resulting crystals have been identified as the octahedral $[Zn(^{t}Bu_2bipy)_2][OTf]_2$ salt by-product (**Figure 3**); similar to the Mg salt as mentioned previously.

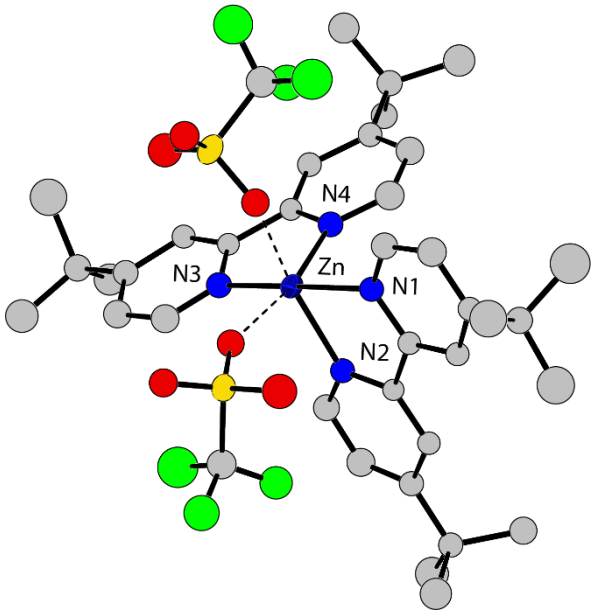

Figure 3. Preliminary solid-state structure of $[Zn(^{t}Bu_2bipy)_2][OTf]_2$. Data set only partially completed, therefore only connectivity can be determined

When **[1]$^{3+}$** was combined with Na, the pale-yellow solution immediately turned to a very deep opaque orange. A $^{31}P\{^{1}H\}$ NMR spectroscopy sample was taken immediately and multiple chemical shifts were observed, with the major shift belonging to **[1]$^{3+}$**. A $^{31}P\{^{1}H\}$ NMR spectrum was obtained over 16 hr and the resulting NMR spectrum contained nine separate chemical shifts. From this, the resulting product cannot be identified.

Table 5. Reduction of [1]$^{3+}$ with Various Reagents

Entry	Reagent	Solvent	Heated temp. (°C); time (hr)	$^{31}P\{^{1}H\}$ NMR δ (ppm)	Assignment
1	2Mg	MeCN	-	238.3(d), 84.9 (t)	**[2]$^{5+}$**
2	$SbPh_3$	MeCN	75; 16	30.6	**[1]$^{3+}$**
3	2($SbPh_3$)	MeCN	75; 32	30.6	**[1]$^{3+}$**
4	2Zn	MeCN	-	113.3	-
5	10($SbPh_3$)	MeCN	-	30.6	**[1]$^{3+}$**
6	2Mg	MeCN	-	236.8(d), 232.7(s)	**[2]$^{5+}$**
7	Se	MeCN	-	30.9	**[1]$^{3+}$**
8	Excess Mg	MeCN	-	238.3(d), 84.9(t)	**[2]$^{5+}$**
9	10Mg	MeCN	-	232.4	-
10	Se	MeCN	75; 62	37.9	-
11	Na	MeCN	-	-	-
12	10Mg	MeCN	-	238.3(d), 84.9(t)	**[2]$^{5+}$**

Reactions were performed at room temperature and were stirred for 1 hr and then assessed by $^{31}P\{^{1}H\}$ NMR spectroscopy. Mixtures were stirred overnight if starting material was still present in the $^{31}P\{^{1}H\}$ NMR spectrum. Mixtures were then heated if starting material was still present in the $^{31}P\{^{1}H\}$ NMR spectrum. For reactions with 2 equivalents of Mg or Zn, 3 equivalents of **[1]$^{3+}$** were used. Assignments of **[1]$^{3+}$** indicate no reaction. Assignments of – indicate that the resulting compound cannot be determined/peak cannot be assigned.

2.7 Experimental

Reagents and Apparatus. All reagents were handled in an Innovative Technology, Inc. (*it*) System One Glovebox (dry N_2) or on a grease-free dual manifold N_2 and vacuum (base vacuum = 2 x 10^{-2} mbar) Schlenk line. Solvents were dried over Na (Et_2O) or CaH_2 (CH_2Cl_2) and then distilled. Anhydrous grade MeCN was obtained from Sigma-Aldrich and used without purification. Prior to use, all solvents were stored for at least 48 hr over 3 Å molecular sieves (MeCN) or 4 Å molecular sieves (Et_2O and CH_2Cl_2), which had been freshly activated at 300 ºC under dynamic vacuum for 48 hr. Deuterated solvents were dried over their corresponding size molecular sieves and were stored for at least 48 hr. TMSOTf (99 %) was distilled before use, 4-methyldiaminopyridine was purified by sublimation under vacuum at 60 ºC, $SPCy_3$ was synthesized according to literature procedure[42] and all other reagents, unless specified, were obtained from Sigma-Aldrich and used without further purification. Reactions were carried out inside the glovebox in screw-cap glass vials that had been dried at 250 ºC for at least 1 hr and placed under dynamic vacuum (glovebox antechamber) while still hot. NMR spectra were obtained on a Bruker AVANCE 300 MHz or 360 MHz NMR Spectrometer, field strength is given explicitly with the characterization data for the compounds. ^{1}H, $^{31}P\{^{1}H\}$, and $^{19}F\{^{1}H\}$ NMR spectroscopy chemical shifts were referenced to $SiMe_4$, 85 % H_3PO_4, and $CFCl_3$, respectively. In most cases, the number of signals in ^{1}H, $^{13}C\{^{1}H\}$, $^{31}P\{^{1}H\}$, and $^{19}F\{^{1}H\}$ NMR spectrum match the proposed structures, but definitive assignment of each chemical shift has not been confirmed. Infrared spectra were collected on samples prepared as Nujol mulls between NaCl plates using a Perkin-Elmer Frontier FT-IR spectrometer. Peaks are reported in wavenumbers (cm^{-1}) with intensities (strong, medium, weak) in parentheses, relative to the most intense peak. Melting points were obtained on samples grease-sealed in glass capillaries under dry nitrogen using an electrothermal apparatus. Unless otherwise stated, crystals for single crystal X-ray diffraction studies were obtained from slow diffusion of a layered non-solvent into a saturated solution of the compound. Single crystal X-ray diffraction data were collected on a Bruker D8/APEX II CCD diffractometer at 173 K. All structures were solved by direct methods and refined by full-matrix least squares on F^2 (SHELXL-97 or SHELXL-2013).[43] All non-hydrogen atoms were refined anisotropically while hydrogen atoms were

assigned positions based on the sp^2 or sp^3 hybridization geometries of their attached carbons, and were given thermal parameters 20% greater than those of their parent atoms.

Synthesis of [P(^{t}Bu$_2$bipy)$_2$][OTf]$_3$ ([1]$^{3+}$): To a rapidly stirred suspension of PCl_3 (5.00 mmol, 0.687 g) and AgOTf (15.00 mmol, 3.854 g) in 15 mL of MeCN, ^{t}Bu$_2$bipy (10.00 mmol, 2.684 g) were added in five portions over ten minutes to yield a yellow suspension. The suspension was left to stir for 2 hr in the dark. The orange supernatant was separated *via* filtration and the solvent removed under reduced pressure. The pale-yellow precipitate was collected *via* filtration, washed with CH_2Cl_2 (10 mL), and dried under dynamic vacuum for 2 hr to yield the product as a fine yellow powder. Yield: 3.202 g (63 %); Melting Point: 257 °C dec.; ^{1}H NMR (CD_3CN, 298 K, 300 MHz, δ [ppm]): 1.51 (*s*, 18H), 1.58 (*s*, 18H), 8.05 (pseudo *dt*, 6.9 Hz, 1.7 Hz, 2H), 8.35 (*dd*, 6.3 Hz, 1.7 Hz, 2H), 8.65 (*dd*, 6.9 Hz, 2.3 Hz, 2H), 9.02 (*m* ,4H), 9.17 (*dd*, 6.3 Hz, 2.9 Hz, 2H); ^{13}C{^{1}H} NMR (CD_3CN, 298 K, 75.4 MHz, δ [ppm]): 29.7 (*s*), 30.8 (*s*), 38.5 (*s*), 39.2 (*s*), 123.8 (*q*, $^1J_{CF}$ = 321 Hz), 124.7 (*d*, J_{CP} = 113 Hz), 124.9 (*dt* J_{CP} = 113 Hz), 129.6 (*dt*, J_{CP} = 177.4 Hz), 129.5 (*d*, J_{CP} = 177.4 Hz), 143.8 (*d*, J_{CP} = 3 Hz), 144.6 (*d*, J_{CP} = 13 Hz), 147.4 (*s*), 148.1 (*s*), 175.1 (*d*, J_{CP} = 4 Hz), 178.5 (*d*, J_{CP} = 3 Hz); ^{31}P{^{1}H} NMR (CD_3CN, 298 K, 121.4 MHz, δ [ppm]): 30.6 (*s*); ^{19}F{^{1}H} NMR (CD_3CN, 298 K, 282.2 Hz, δ [ppm]): -79.2 (*s*).

[(Ph$_3$PO)P(^{t}Bu$_2$bipy)$_2$][OTf]$_3$ ([1(OPPh$_3$)]$^{3+}$; 1-3): To a rapidly stirred solution of **[1]$^{3+}$** (0.50 mmol, 0.508 g) in 5 mL of MeCN, $OPPh_3$ (0.50 mmol, 0.139 g) was added. The solution remained a clear yellow. The solution was left to stir for 30 mins, where it became darker. The ^{31}P{^{1}H} NMR spectrum contained three chemical shifts of different intensity, including the starting material peaks. The solution was analysed after 16 hr of stirring at room temperature, turning a clear, dark orange, however it contained 5 signals. ^{31}P{^{1}H} NMR (CD_3CN, 298 K, 121.4 MHz, δ [ppm]): 65.6 (*s*), 56.9 (*d*), 39.2 (*s*), 29.9 (*s*), -23.4 (*d*); ^{19}F{^{1}H} NMR (CD_3CN, 298 K, 282.2 Hz, δ [ppm]): -79.2 (*s*).

[(Ph$_3$PO)P(^{t}Bu$_2$bipy)$_2$][OTf]$_3$ ([1(OPPh$_3$)]$^{3+}$; 1-4): To a rapidly stirred suspension of **[1]$^{3+}$** (0.50 mmol, 0.508 g) in 8 mL of DCM, OPPh$_3$ (0.50 mmol, 0.139 g) was added. The mixture remained cloudy yellow. The solvent was removed under reduced pressure, and the yellow powder was analyzed by NMR spectroscopy. The compound was crystallized from MeCN, forming yellow crystals. However, the crystals were just of the **[1]$^{3+}$** starting material. ^{31}P{^{1}H} NMR (CD$_3$CN, 298 K, 121.4 MHz, δ [ppm]): 65.6 (*s*), 56.9 (*d*), 33.4 (*s*), 29.6 (*s*); ^{19}F{^{1}H} NMR (CD$_3$CN, 298 K, 282.2 Hz, δ [ppm]): -79.2 (*s*).

[(Cy$_3$PS)P(^{t}Bu$_2$bipy)$_2$][OTf]$_3$ ([1(SPCy$_3$)]$^{3+}$; 1-9): To a rapidly stirred suspension of **[1]$^{3+}$** (0.50 mmol, 0.508 g) in 5 mL of MeCN, SPCy$_3$ was added. The yellow solution turned a bright cloudy orange upon addition. The mixture was left to stir for 30 mins and was then analysed by ^{31}P{^{1}H} NMR spectroscopy. The mixture was left to stir for an addition 3 hr, analysed by ^{31}P{^{1}H} NMR spectroscopy, and then again for another 16 hr. Each spectrum was analysed and stirring continued until the **[1]$^{3+}$** starting material chemical shift disappeared. The solvent was removed under reduced pressure and the pale orange powder was analysed by ^{31}P{^{1}H} NMR spectroscopy. A recrystallization was set up in MeCN, however only orange powder was recovered. ^{1}H NMR (CD$_3$CN, 298 K, 300 MHz, δ [ppm]): 9.59 (*dt*, 6.7 Hz, 2.2 Hz, 2H), 8.97 (*d*, 1.5 Hz, 2H), 8.80 (*dd*, 5.3 Hz, 0.6 Hz, 3H), 8.49 – 8.46 (*m*, 6H), 8.65 (*dd*, 4.1 Hz, 1.9 Hz, 3H), 1.53 (*s*, 20H), 1.48 (*s*, 30H); ^{31}P{^{1}H} NMR (CD$_3$CN, 298 K, 121.4 MHz, δ [ppm]): 138.9 (*s*), 104.1 (*s*), 90.5 (*d*, 31.4 Hz), 62.1 (*s*); ^{19}F{^{1}H} NMR (CD$_3$CN, 298 K, 282.2 Hz, δ [ppm]): -79.2 (*s*).

[MeP(ᵗBu₂bipy)₂][OTf]₃ ([1(Me)]³⁺; 2-2): To a rapidly stirred suspension of **[1]**$^{3+}$ (0.54 mmol, 0.547 g) in 5 mL of MeCN, MeOTf was added. After 15 minutes, the cloudy yellow mixture turned into a thick slurry. A sample was analysed by $^{31}P\{^{1}H\}$ NMR spectroscopy and then the reaction was left to stir for overnight. The mixture was left to settle, and the colourless crystalline powder was analysed by $^{31}P\{^{1}H\}$ NMR spectroscopy. The compound was dried under reduced pressure and then washed three times with diethyl ether. The isolated powder was analysed by heteronuclear NMR spectroscopy. ^{1}H NMR (CD_3CN, 298 K, 300 MHz, δ [ppm]): 9.35 – 9.31 (*m*, 2H), 9.19 (*dt*, 7.9 Hz, 0.9 Hz, 2H), 9.00 (*td*, 8.0 Hz, 1.1 Hz, 2H), 7.88 – 7.82 (*m*, 1H), 7.76 – 7.58 (*m* ,4H); $^{13}C\{^{1}H\}$ NMR (CD_3CN, 298 K, 75.4 MHz, δ [ppm]): 151.1 (*s*), 146.3 (*d*, J_{CP} = 22Hz), 138.8 (*s*), 136.3 (*d*, J_{CP} = 31 Hz), 132.9 (*d*, J_{CF} = 2 Hz), 131.8 (*d*, J_{CP} = 12 Hz), 127.8 (*d*, J_{CP} = 4 Hz); $^{31}P\{^{1}H\}$ NMR (CD_3CN, 298 K, 121.4 MHz, δ [ppm]): 136.8 (*s*); $^{19}F\{^{1}H\}$ NMR (CD_3CN, 298 K, 282.2 Hz, δ [ppm]): -79.3 (*s*).

[(NBN)P(ᵗBu₂bipy)₂][OTf]₃ ([1(NBN)]³⁺; 3-2): To a rapidly stirred suspension of **[1]**$^{3+}$ (0.54 mmol, 0.547 g) in 5 mL of MeCN, NBN (0.718 mmol, 0.068 g) was added. After 4.5 hr, the clear yellow mixture was analyzed by $^{31}P\{^{1}H\}$ NMR spectroscopy, revealing the only chemical shift to be the **[1]**$^{3+}$ starting material. The compound was heated in a reaction bomb for 4 hr and assessed by $^{31}P\{^{1}H\}$ NMR spectroscopy again. Another equivalent of NBN was added and was heated for another 16 hr. A sample was assessed by $^{31}P\{^{1}H\}$ NMR spectroscopy again, and then another equivalent was added. The mixture was heated again overnight, producing a red-orange solution. The solvent was removed under reduced pressure and the brown-red solid was washed three times with diethyl ether and was analysed. Yield: 0.283 g (36%). Attempts were made to crystallize in minimal amounts of MeCN, however the only recovered crystals were assigned to protonated $^{t}Bu_2$bipy.

[(NBD)P(ᵗBu₂bipy)₂][OTf]₃ ([1(NBD)]³⁺; 3-3): To a rapidly stirred suspension of **[1]**$^{3+}$ (0.50 mmol, 0.512 g) in 5 mL of MeCN, NBD (0.50 mmol, 50.8 µL) was added. After 1 hr, the clear yellow mixture was analyzed by $^{31}P\{^{1}H\}$ NMR spectroscopy, revealing the only chemical shift to be the **[1]**$^{3+}$ starting material. The compound was heated in a reaction bomb for 16 hr at 75 °C and assessed by $^{31}P\{^{1}H\}$ NMR spectroscopy again, revealing a new chemical shift. The solvent was removed under reduced pressure and the brown-red solid was washed three times with diethyl ether solid was analysed. Attempts were made to crystallize in minimal amounts of MeCN, however the only recovered crystals were assigned to protonated $^{t}Bu_2$bipy.

[Cl₂P(ᵗBu₂bipy)₂][OTf]₃ ([1(Cl₂)]³⁺; 4-1): Dissolved **[1]**$^{3+}$ (0.50 mmol, 0.510 g) in 5 mL of MeCN in a 250 mL Schlenk Flask in the glovebox. The flask was brought out of the glovebox and attached to a Schlenk Line. Added 1 mL SO_2Cl_2 (1 molar in DCM) in excess to the Schlenk flask, turning the clear yellow solution quickly to a colourless mixture. The solvent was removed under reduced pressure and the colourless powder was analysed by $^{31}P\{^{1}H\}$ NMR spectroscopy. Attempts were made to crystallize in minimal amounts of MeCN and layered with 1 mL of diethyl ether, however the only recovered crystals were assigned to protonated $^{t}Bu_2$bipy.

[Br₂P(ᵗBu₂bipy)₂][OTf]₃ ([1(Br₂)]³⁺; 4-6): Dissolved **[1]**$^{3+}$ (0.50 mmol, 0.510 g) in 5 mL of MeCN in a 250 mL Schlenk Flask in the glovebox. The flask was brought out of glovebox and attached to a Schlenk Line. Added 0.05 mL Br_2 in excess to the Schlenk flask, turning the clear yellow solution quickly to a deep dark orange. The mixture was left to stir for 20 minutes, then the solvent was removed under reduced pressure, and the light orange powder was analysed by $^{31}P\{^{1}H\}$ NMR spectroscopy. Multiple chemical shifts were observed in the $^{31}P\{^{1}H\}$ NMR spectrum, with the major peak assigned to the hydrolysis product.[37]

[(pico)P(ᵗBu₂bipy)₂][OTf]₃ ([1(pico)]³⁺; 4-3): To a rapidly stirred suspension of **[1]**$^{3+}$ (0.50 mmol, 0.496 g) in 5 mL of MeCN, 4-picoline-N-oxide (0.50 mmol, 0.055 g) was added forming a clear deep red solution. The mixture was assessed by $^{31}P\{^{1}H\}$ NMR spectroscopy and the solvent was immediately removed under reduced pressure and a dark brown solid was obtained. Attempts were made to crystallize the compound in minimal amounts of MeCN and layered with 1 mL of diethyl ether, however no crystals were obtained.

[P₃(ᵗBu₂bipy)₂][OTf]₅ ([2]⁵⁺; 5-1): To a rapidly stirred suspension of **[1]**$^{3+}$ (0.41 mmol, 0.415 g) in 5 mL of MeCN, Mg (0.27 mmol, 0.007 g) was added forming a deep orange after 20 minutes. The mixture was stirred for 1 hr, and a sample was filtered and assessed by $^{31}P\{^{1}H\}$ NMR spectroscopy. The mixture was left to stir for another 24 hr, where it was assessed by $^{31}P\{^{1}H\}$ NMR spectroscopy again. The excess Mg was filtered off and the resulting solvent from the clear brown orange solution was removed under reduced pressure. The solid was assessed by $^{31}P\{^{1}H\}$ NMR spectroscopy and was crystallized in minimal amounts of MeCN, layered with 1 mL of diethyl ether, and placed in the freezer at -26 °C. However, the only recovered crystals were assigned to protonated $^{t}Bu_2$bipy and the Mg salt by-product.

[P₃(ᵗBu₂bipy)₂][OTf]₅ ([2]⁵⁺; 5-4): To a rapidly stirred suspension of **[1]**$^{3+}$ (0.41 mmol, 0.415 g) in 5 mL of MeCN, Zn powder (0.33 mmol, 0.022 g) was added forming a cloudy green mixture after 10 minutes. Stirred the mixture for 1 hr, and a sample was filtered and assessed by $^{31}P\{^{1}H\}$ NMR spectroscopy. The mixture was left to stir for another 24 hr, where it was assessed by $^{31}P\{^{1}H\}$ NMR spectroscopy again, showing no change. The mixture was stirred for another 48 hr, and a sample was filtered and assessed by $^{31}P\{^{1}H\}$ NMR spectroscopy, showing the presence of a new chemical shift. The excess Zn was filtered off and the resulting clear green solution was placed in a freezer at -26 °C and left to recrystallize. Off-yellow crystals were isolated; however, the crystals were assigned to the Zn salt by-product.

[P_3(^{t}Bu_2bipy)$_2$][OTf]$_5$ ([2]$^{5+}$; 5-11): To a rapidly stirred suspension of **[1]$^{3+}$** (0.41 mmol, 0.415 g) in 5 mL of MeCN, freshly cut Na chunks (0.50 mmol, 0.012 g) were added forming a deep orange after 5 minutes. A sample was immediately filtered and assessed by $^{31}P\{^1H\}$ NMR spectroscopy, showing the presence of multiple chemical shifts, but none that matched the desired product **[2]$^{5+}$**. The mixture was left to stir for another 24 hr, where it was assessed by $^{31}P\{^1H\}$ NMR spectroscopy again, showing no change.

The following tables summarize the attempted syntheses of other [P]$^{3+}$ complexes with varying ligands (**Table 6**) as well as reactions using **[1(Cl$_2$)]$^{3+}$** (**Table 7**). The development of new P(III) centred tricationic complexes is ongoing and preliminary experiments have been conducted and will be discussed in **Chapter 5**.

General procedure for Table 6: To a rapidly stirring solution of PCl_3 and Reagent B in 5 mL solvent, Reagent C was slowly added. The mixture was assessed by $^{31}P\{^1H\}$ NMR spectroscopy immediately after addition, and was left stirring for 1 hr. The mixture was assessed again by $^{31}P\{^1H\}$ NMR, and left to stir overnight if no change was observed in the $^{31}P\{^1H\}$ NMR spectrum. This process is repeated if necessary.

Table 6. Synthesis of $[1]^{3+}$ and Other $[P]^{3+}$ complexes

Entry	Reagent B	Reagent C	Solvent	$^{31}P\{^1H\}$ NMR δ (ppm)	Assignment
1	3AgOTf	2bipy	MeCN	35.5	**$[P(bipy)_2][OTf]_3$**
2	3AgOTf	2^{t}Bu$_2$bipy	MeCN	30.8	**$[1]^{3+}$**
3	3AgOTf	3DMAP	MeCN	102.3	**$[P(DMAP)_3][OTf]_3$**
4	3AgOTf	2^{t}Bu$_2$bipy	MeCN	30.6	**$[1]^{3+}$**
5	3AgOTf	3Pyr	MeCN	-	-
6	3AgOTf	2^{t}Bu$_2$bipy	MeCN	30.6	**$[1]^{3+}$**
7	3AgOTf	^{Me}PDI	MeCN	34.5	**$[P(^{Me}PDI)_2][OTf]_3$**
8	3.5TMSOTf	^{Me}PDI	MeCN	-	-
9	4TMSOTf	4 ^{dipp}DAB	DCM	-	-
10	4TMSOTf	$BimEt_3$	DCM	-	-
11	3.5TMSOTf	BIAN	DCM	232.9	**$[P(BIAN)][OTf]_3$**
12	$PPyr_3$	3TMSOTf	DCM	-	-
13	$PPyr_3$	3TMSOTf	MeCN	-	-
14	4TMSOTf	$BimEt_3$	MeCN	56.1	**$[P(BimEt_3)][OTf]_3$**

Reactions were performed at room temperature and were stirred for 1 hr and then assessed by $^{31}P\{^1H\}$ NMR spectroscopy. Mixtures were stirred overnight if starting material was still present in the $^{31}P\{^1H\}$ NMR spectrum. Assignments of – indicate that the resulting compound cannot be determined/peak cannot be assigned.

General procedure for Table 7: To a rapidly stirring mixture of **[1(Cl$_2$)]$^{3+}$** in 5 mL of solvent, Reagent B was slowly added. The mixture was assessed by $^{31}P\{^1H\}$ NMR spectroscopy immediately after addition, and was left stirring for 1 hr. The mixture was assessed again by $^{31}P\{^1H\}$ NMR, and depending on the result, further action was taken. If the NMR spectrum showed no change in chemical shifts, then the mixture was placed into a reaction bomb and was heated for 16 h at 75 °C. If the $^{31}P\{^1H\}$ NMR spectrum showed a slight change, then the heating was repeated.

Table 7. Reactions [1(Cl$_2$)]$^{3+}$ with Various Reagents

Entry	Reagent B	Reagent C	Solvent	Heated temp. (°C); time (hr)	$^{31}P\{^1H\}$ NMR δ (ppm)	Assignment
1	$SbPh_3$	-	MeCN	-	30.6	**[1]$^{3+}$**
2	NaOMe	-	MeCN	75; 16	-10.8	-
3	TMSOTf	-	MeCN	-	-146.9	**[1(Cl$_2$)]$^{3+}$**
4	TMSOTf	^{t}Bu$_2$bipy	MeCN	-	-142.2	**[1(Cl$_2$)]$^{3+}$**
5	AgOTf	-	MeCN	-	-146.9	**[1(Cl$_2$)]$^{3+}$**
6	AgOTf	^{t}Bu$_2$bipy	MeCN	-	-146.9	**[1(Cl$_2$)]$^{3+}$**
7	2TMSOTf	bipy	MeCN	-	-142.2	**[1(Cl$_2$)]$^{3+}$**
8	2TMSOTf	2DMAP	MeCN	75; 48	-146.9	**[1(Cl$_2$)]$^{3+}$**
9	NaOMe	-	MeCN	75; 48	-146.9	**[1(Cl$_2$)]$^{3+}$**

Reactions were performed at room temperature and were stirred for 1 hr and then assessed by $^{31}P\{^1H\}$ NMR spectroscopy. Mixtures were stirred overnight if starting material was still present in the $^{31}P\{^1H\}$ NMR spectrum. Mixtures were then heated if starting material was still present in the $^{31}P\{^1H\}$ NMR spectrum. Assignments of – indicate that the resulting compound cannot be determined/peak cannot be assigned.

Chapter 3. P(III) Centred Dicationic Complexes

3.1 Introduction

There are many examples of mononuclear dicationic main group complexes, with a variety of ligands being used to stabilize these highly reactive compounds. Phosphorus centred dicationic complexes have been reported with monodentate ligands[44–46], chelating ligands[47–49], carbene ligands[34,50–53], carbone ligands[51], and with numerous examples using phosphine ligands.[44,54–58] Recent developments in the Burford group reported the synthesis and isolation of *bis*-triflate salts of 2-phosphino-1,3-diphosphonium cationic complexes[56,57] (**Scheme 31**).

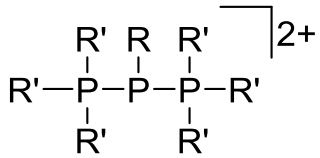

R = Cy, ^{t}Bu, Me, N^{i}Pr$_2$, R' = Me

Scheme 31. General structure for 2-phosphino-1,3-diphosphonium dicationic complex

As mentioned in **Chapter 1**, charged phosphorus centres dramatically influence their reactivities, enabling comprehensive studies of their structure and bonding. To further develop this library of growing main group polycationic complexes, four new $[PhP]^{2+}$ dicationic complexes (**$[3L]^{2+}$**: where L = ligand bound to P(III) centre) have been isolated (**Scheme 32**). A full list of all reactions for the synthesis of these **$[3L]^{2+}$** complexes are summarized in **Tables 10 – 14**. Similarly, to **$[1]^{3+}$** discussed in **Chapter 2**, their future in catalysis and small molecule activation, coupled with their simplistic synthesis, will be integral in this developing field of main group chemistry.

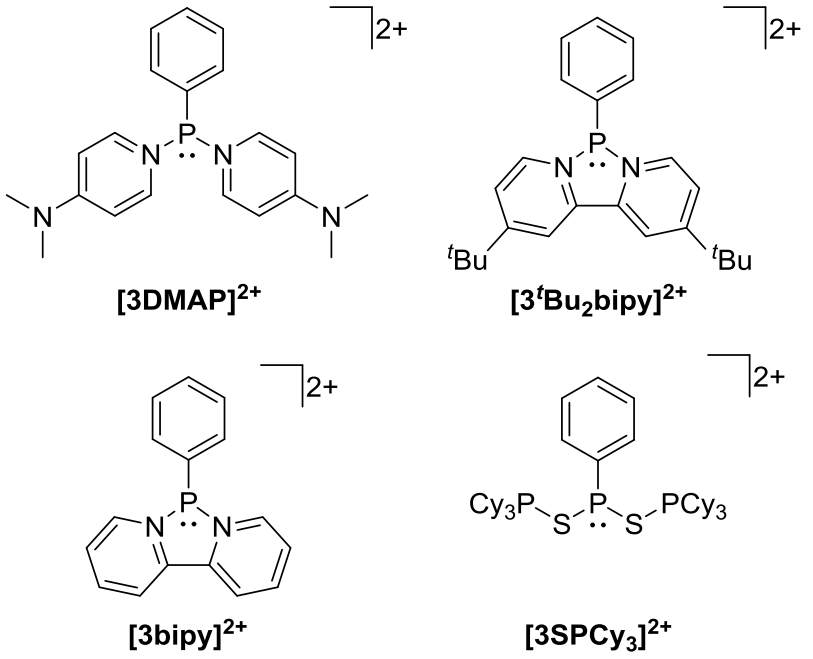

Scheme 32. Newly synthesised **[3L]**$^{2+}$ complexes

In all cases, the magnitude of the positive charge on the complex is balanced by an equivalent number of OTf anions. These **[3L]**$^{2+}$ complexes can be envisaged as two neutral ligands donating onto a positively charged $[RP]^{2+}$ acceptor.[56] This can be envisaged for other reported complexes such as the previously mentioned 2-phosphino-1,3-diphosphonium dicationic complex, and the *bis*-carbene derivative $[(NHC)_2PR]^{2+}$, where they show similar trigonal pyramidal geometries and use triflate as the counter anions (**Scheme 33**).[51]

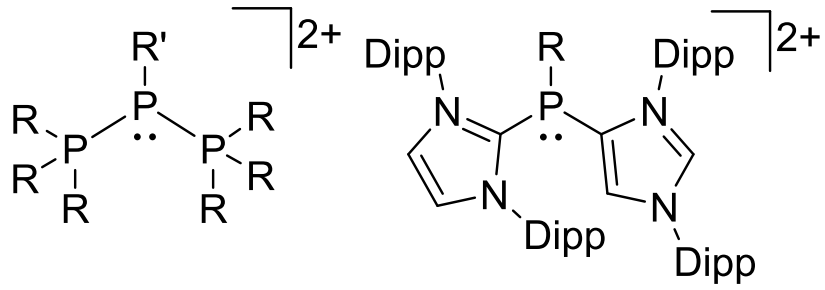

Scheme 33. Ligand coordination modes on a $[RP]^{2+}$ acceptor (left) and a *bis*-carbene dicationic complex R = H, Me (right)

A one-pot synthesis is used for the formation of the **[3L]$^{2+}$** complexes (**Scheme 34**), where the phosphorus containing starting material ($RPCl_2$) is combined with the ligand and the halide abstractor all in one step. In previous reports, the halide abstractor used in the synthesis of various dicationic complexes was $AlCl_3$.[56,57,59] However, it was found that the resulting counter anion, $AlCl_4$, reacted with incoming reagents when used in new reactions. To ensure that further reactions using the dicationic complex occur only at the phosphorus centre and not with the counter anion, TMSOTf has been selected as the halide abstractor. The formation of TMSCl drives the reaction towards completion and can be easily removed under reduced pressure, also making TMSOTf an optimal choice.

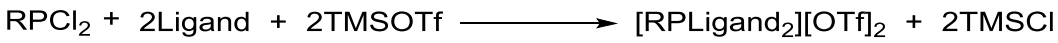

Scheme 34. General synthesis of **[3L]$^{2+}$** complexes

In this case, the **[3L]$^{2+}$** complexes have R = Ph. There are examples of phosphorus centred dicationic complexes having phenyl as a substituent, however, attempts to synthesise the phenyl derivative of the 2-phosphino-1,3-diphosphonium dicationic complexes previously mentioned in **Scheme 31** have led to the formation of $[R'_3P\text{-}P(R)\text{-}P(R)\text{-}PR'_3][OTf]_2$ through a redox process.[56] (**Scheme 35**)

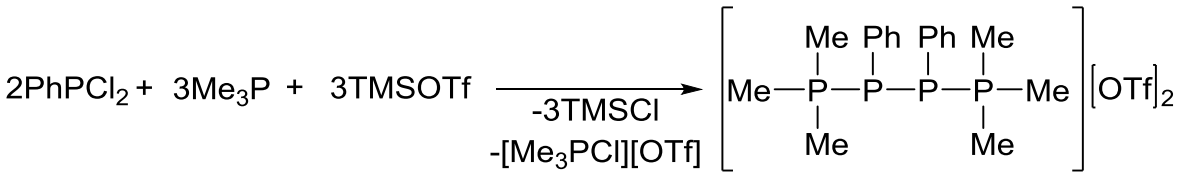

Scheme 35. Product obtained in the attempted synthesis of phenyl derivative of 2-phosphino-1,3-diphosphonium dicationic complex

However, with the new **[3L]$^{2+}$** complexes, oxidation of the ligand does not occur, likely due to the high oxidative resistance seen with bipy, ^{t}Bu$_2$bipy, DMAP, and SPCy$_3$ as discussed in **Chapter 1**.

The synthesis of the **[3L]$^{2+}$** complexes were performed in DCM and the solids were crystallized in minimal amounts of MeCN and layered with 1 mL of diethyl ether. A stoichiometry of one equivalent of $PhPCl_2$ to two equivalents of the ligand to two equivalents of TMSOTf were attempted for the synthesis of **[3DMAP]$^{2+}$**, and **[3SPCy$_3$]$^{2+}$** and a stoichiometry of 1:1:2 was attempted for the synthesis of **[3^{t}Bu$_2$bipy]$^{2+}$**, and **[3bipy]$^{2+}$**. These stoichiometries left a significant amount of $PhPCl_2$ leftover, as observed in the $^{31}P\{^{1}H\}$ NMR spectrum. The optimized ratios were found to be 1:2.5:2.5 for monodentate ligands and 1:1.5:2.5 for bidentate ligands as seen in **Scheme 36**; this resulted in the absence of the starting material $PhPCl_2$ chemical shift from the $^{31}P\{^{1}H\}$ NMR spectrum, indicating a full conversion. After 1 hr of stirring, the compounds were isolated as colourless solids, washed three times with diethyl ether, and then recrystallized in MeCN. See the appendix for full crystal data.

$$PhPCl_2 + 2.5Ligand + 2.5TMSOTf \xrightarrow[-0.5TMSOTf]{-0.5Ligand} [RPLigand_2][OTf]_2 + 2TMSCl$$

$$PhPCl_2 + 1.5Ligand + 2.5TMSOTf \xrightarrow[-0.5TMSOTf]{-0.5Ligand} [RPLigand][OTf]_2 + 2TMSCl$$

Scheme 36. Equations for the syntheses of the **[3L]$^{2+}$** complexes

3.2 $[3L]^{2+}$ where L = DMAP, $^{t}Bu_2$bipy, and bipy

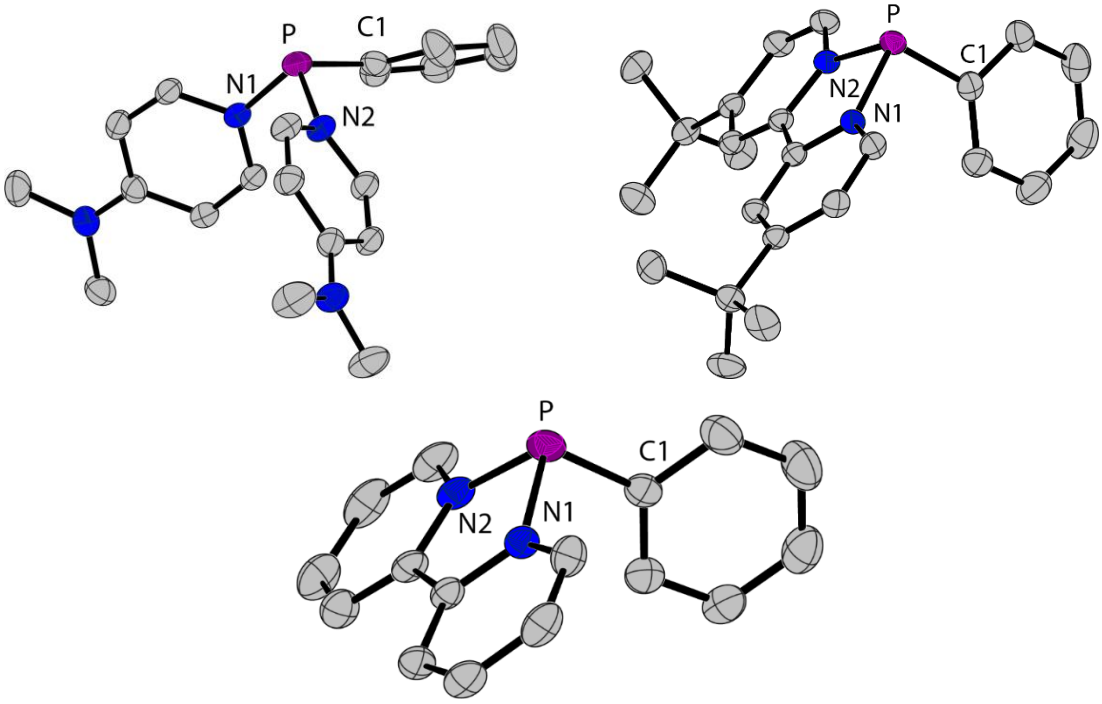

Figure 4. Solid-state structure of **[3DMAP]**$^{2+}$ and **[3^{t}Bu$_2$bipy]**$^{2+}$ (top), and **[3bipy]**$^{2+}$ (bottom)

Ellipsoids are shown at 50% probability. Hydrogen atoms, triflate anions and solvent molecules have been omitted for clarity. The sum of the angles around the central phosphorus atom is less than 360 ° for **[3DMAP]**$^{2+}$: 301°, **[3^{t}Bu$_2$bipy]**$^{2+}$: 281°, and **[3bipy]**$^{2+}$: 285°; **Table 8**), indicating that the lone pair on the phosphorus is stereochemically active, and that the geometry of the phosphorus centre is best described as a trigonal pyramid. The interaction between the phosphorus centre and the closest triflate anion is outside the sum of the O-P covalent radii ($\Sigma_{r,cov}$(O, P) = 1.74 Å)[40], but inside the sum of the van der Waals radii ($\Sigma_{r,vdW}$(O, P) = 3.32 Å)[41] for all three **[3L]**$^{2+}$ complexes, meaning the compounds are best described as *bis*-triflate salts of a phosphorus dication.

Both N-P bond lengths of **[3DMAP]$^{2+}$** are indistinguishable and are significantly shorter than the N-P bond lengths of **[3bipy]$^{2+}$** and **[3^{t}Bu$_2$bipy]$^{2+}$**. This indicates a stronger N-P bond, which corresponds to DMAP being a stronger σ donor than the bipyridine ligands, likely due to resonance structures possible for DMAP (**Scheme 37**).

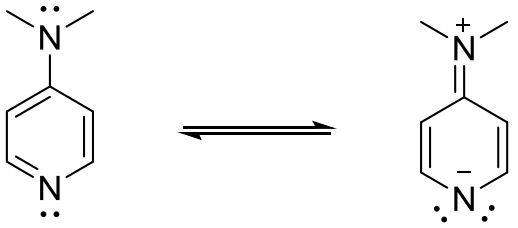

Scheme 37. Resonance structure of DMAP, making it a stronger σ donor

When compared to other nitrogen stabilized dicationic complexes such as the *bis*[(dialkylamino)cyclopropenimine]-stabilized [PhP]$^{2+}$ complexes (**[4a]$^{2+}$** and **[4b]$^{2+}$**) shown in **Scheme 38**[49] and the *bis*(pyrazolyl)borate-stabilized [PhP]$^{2+}$ complex (**[5]$^{2+}$**) shown in **Scheme 39**[33], the N-P bond lengths of the chelating **[3L]$^{2+}$** complexes are slightly longer. This is likely due to the additional donating groups on the ligands of **[4a]$^{2+}$** and **[4b]$^{2+}$**. N-P bond lengths of **[3DMAP]$^{2+}$** are comparable to **[5]$^{2+}$**.

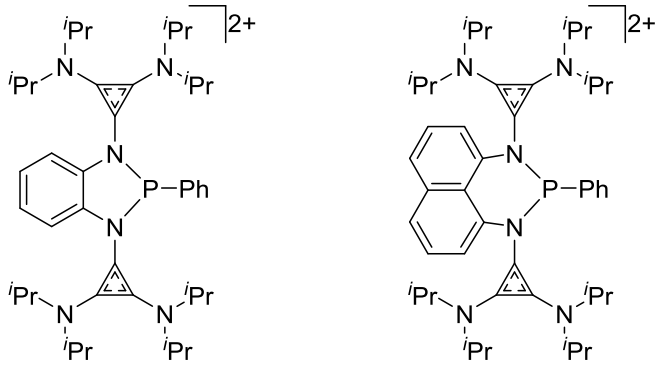

[4a]$^{2+}$ **[4b]$^{2+}$**

Scheme 38. *Bis*[(dialkylamino)cyclopropenimine]-stabilized [PhP]$^{2+}$ centred dicationic complexes[49]

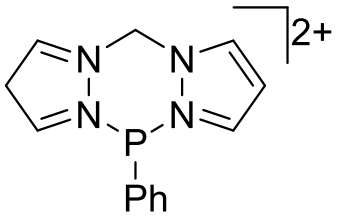

[5]$^{2+}$

Scheme 39. *Bis*(pyrazolyl)borate-stabilized [PhP]$^{2+}$ centred dicationic complex[33]

Table 8. Structural Parameters of [3DMAP]$^{2+}$, [3^{t}Bu$_2$bipy]$^{2+}$, and [3bipy]$^{2+}$ Compared to Other [PhP]$^{2+}$ Derivatives

Bond(s)	[3DMAP]$^{2+}$	[3^{t}Bu$_2$bipy]$^{2+}$	[3bipy]$^{2+}$	[4a]$^{2+}$	[4b]$^{2+}$	[5]$^{2+}$
P1-N1	1.761(4)	1.7962(13)	1.8087(19)	1.768(2)	1.725(2)	1.758(1)
P1-N2	1.764(4)	1.8069(14)	1.805(2)	1.762(2)	1.727(2)	1.769(1)
P1-C1	1.813(5)	1.8182(17)	1.805(2)	1.820(3)	1.828(3)	1.819(2)
N1-P-N2	98.7(2)	85.14(6)	85.30(9)	90.21(8)	96.6(1)	92.01(7)
N1-P-C1	99.8(2)	100.75(7)	100.78(9)	101.22(9)	100.2(1)	100.48(7)
N2-P-C1	102.2(2)	94.36(7)	97.57(10)	100.49(9)	98.1(1)	97.23(7)

Bond lengths in Å and bond angles in °.

All of the dicationic compounds described contain a trigonal pyramidal geometry, clearly indicating the presence of a stereochemically active lone pair on the phosphorus centre.[60]

3.3 $[3L]^{2+}$ where L = $SPCy_3$

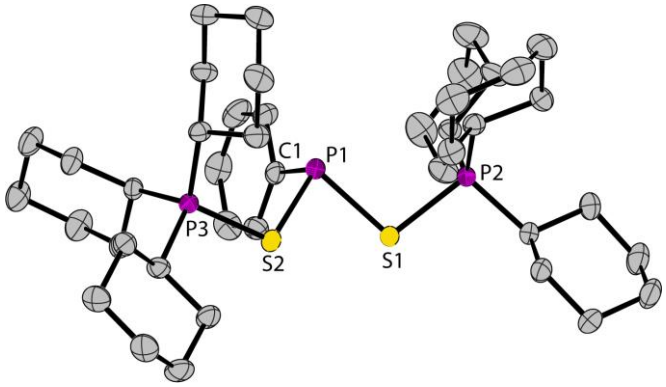

Figure 5. Solid-state structure of **$[3SPCy_3]^{2+}$**

Ellipsoids are shown at 50% probability. Hydrogen atoms, triflate anions and solvent molecules have been omitted for clarity. The sum of the angles around the phosphorus atom is 291°, less than 360 °, indicating that the lone pair on the phosphorus is stereochemically active, making the molecule's geometry trigonal pyramidal (**Table 9**). The interaction between the phosphorus centre and the closest triflate anion is outside the sum of the O-P van der Waals radii ($\Sigma_{r,vdW}$(O, P) = 3.40 Å)[41]: 4.680(2) Å, meaning the compound is best described as a *bis*-triflate salt of a phosphorus dication. The interaction between S1/S2 and the closest triflate anion is also outside the sum of the O-S van der Waals radii ($\Sigma_{r,vdW}$(O, S) = 3.39 Å)[41]: 4.416(2) Å and 3.444(2) Å respectively.

The S1-P2 and S2-P3 bond lengths in **$[3SPCy_3]^{2+}$** are 2.0815(7) Å and 2.0785(7) Å respectively and are significantly longer compared to the S-P bond length in the starting material $SPCy_3$ (1.966(5) Å)[61], implying that the bonds in the complex are weaker, presumably to balance the electron density loss on sulfur. A similar trend has recently been shown in other donor-acceptor complexes of phosphine chalcogenides with As and Sb.[62,63]

Although no other example of a cationic P-S-P-S-P complex is known, when compared to the S-P1 bonds of the neutral compound *bis*(4-methylbenzoylthio)-phenylphosphine[64] (**[6]**; **Scheme 40**), the S-P1 bonds of **$[3SPCy_3]^{2+}$** are slightly longer. This is likely due to the steric hindrance of the Cy rings of the $SPCy_3$ moieties of **$[3SPCy_3]^{2+}$**.

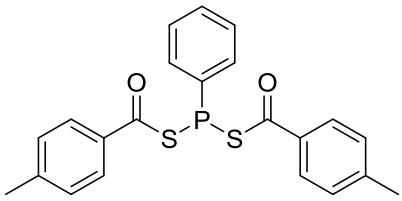

[6]

Scheme 40. The neutral compound *bis*(4-methylbenzoylthio)phenylphosphine[64]

Table 9. Structural Parameters of $[3SPCy_3]^{2+}$ Compared to [6] and $SPCy_3$

Bond(s)	$[3SPCy_3]^{2+}$	[6]	$SPCy_3$
P1-S1	2.1638(7)	2.146(2)	1.9579(6)
P1-S2	2.1586(7)	2.145(2)	
P1-C1	1.814(2)	1.825(5)	
P2-S1	2.0815(7)		
P3-S2	2.0785(7)		
P1-S2-P3	107.46(3)		
P1-S1-P2	100.55(3)		
S2-P1-C1	103.92(7)	102.3(2)	
S2-P1-S1	85.93(3)	91.41(6)	
S1-P1-C1	100.87(8)	101.4(2)	

Bond lengths in Å and bond angles in °

The $SPCy_3$ ligand is a weaker donor when compared to ligands based on the pyridine framework. As such, $SPCy_3$ should be more labile in solution, potentially opening a coordination site at the phosphorus centre, facilitating further reactivity.

3.4 Experimental

Reagents and Apparatus. All reagents were handled in an Innovative Technology, Inc. (*it*) System One Glovebox (dry N_2) or on a grease-free dual manifold N_2 and vacuum (base vacuum = 2 x 10^{-2} mbar) Schlenk line. Solvents were dried over Na (Et_2O) or CaH_2 (CH_2Cl_2) and then distilled. Anhydrous grade MeCN was obtained from Sigma-Aldrich and used without purification. Prior to use, all solvents were stored for at least 48 hr over 3 Å molecular sieves (MeCN) or 4 Å molecular sieves (Et_2O and CH_2Cl_2), which had been freshly activated at 300 ºC under dynamic vacuum for 48 hr. Deuterated solvents were dried over their corresponding size molecular sieves and were stored for at least 48 hr. TMSOTf (99 %) was distilled before use, 4-methyldiaminopyridine was purified by sublimation under vacuum at 60 ºC, $SPCy_3$ was synthesized according to literature procedure[42] and all other reagents, unless specified, were obtained from Sigma-Aldrich and used without further purification. Reactions were carried out inside the glovebox in screw-cap glass vials that had been dried at 250 ºC for at least 1 hr and placed under dynamic vacuum (glovebox antechamber) while still hot. NMR spectra were obtained on a Bruker AVANCE 300 MHz or 360 MHz NMR Spectrometer, field strength is given explicitly with the characterization data for the compounds. ^1H, $^{31}P\{^1H\}$, and $^{19}F\{^1H\}$ NMR spectroscopy chemical shifts were referenced to $SiMe_4$, 85 % H_3PO_4, and $CFCl_3$, respectively. In most cases, the number of signals in ^1H, $^{13}C\{^1H\}$, $^{31}P\{^1H\}$, and $^{19}F\{^1H\}$ NMR spectrum match the proposed structures, but definitive assignment of each chemical shift has not been confirmed. Infrared spectra were collected on samples prepared as Nujol mulls between NaCl plates using a Perkin-Elmer Frontier FT-IR spectrometer. Peaks are reported in wavenumbers (cm^{-1}) with intensities (strong, medium, weak) in parentheses, relative to the most intense peak. Melting points were obtained on samples grease-sealed in glass capillaries under dry nitrogen using an electrothermal apparatus. Unless otherwise stated, crystals for single crystal X-ray diffraction studies were obtained from slow diffusion of a layered non-solvent into a saturated solution of the compound. Single crystal X-ray diffraction data were collected on a Bruker D8/APEX II CCD diffractometer at 173 K. All structures were solved by direct methods and refined by full-matrix least squares on F^2 (SHELXL-97 or SHELXL-2013).[43] All non-hydrogen atoms were refined anisotropically while hydrogen atoms were assigned positions based on the sp^2 or sp^3 hybridization geometries of their attached carbons,

and were given thermal parameters 20% greater than those of their parent atoms. A sample of **[PhP(ᵗBu$_2$bipy)][OTf]$_2$** was analyzed by Canadian Microanalytical Service Ltd. in Delta, British Columbia, Canada, for elemental analysis. The purity of the characterized compounds is evident from a sharp melting point range, coupled with chemical shifts that correspond to the single compound in the $^{31}P\{^1H\}$ NMR spectrum.

[PhP(bipy)][OTf]$_2$ ([3bipy]$^{2+}$; 10-2): To a rapidly stirring solution of $PhPCl_2$ (1.00 mmol, 0.179 g) and TMSOTf (2.00 mmol, 0.445 g) in 5 mL DCM, $^tBu_2$bipy (1.00 mmol, 0.268 g) was added, producing a pale-yellow solution. The solution was stirred for 1 hr and then checked by $^{31}P\{^1H\}$ NMR spectroscopy. The solvent was removed under reduced pressure and washed with diethyl ether three times. The colourless powder product was crystallized from MeCN at -26 ˚C. Yield: 0.4274 g (76 %); Melting Point: 218 °C dec.; ^1H NMR (CD_3CN, 298 K, 300 MHz, δ [ppm]): 9.38 – 9.35 (*m*, 2H, bipy), 9.20 (*dt*,1 Hz, 8 Hz, 2H, bipy), 9.00 (*td*, 1 Hz, 8 Hz, 2H, bipy), 8.41 – 8.37 (*m*, 2H, bipy), 7.87 – 7.58 (*m*, 5H, Ph); $^{13}C\{^1H\}$ NMR (CD_3CN, 298 K, 75.4 MHz, δ [ppm]): 151.1 (*s*, bipy), 146.3 (*d*, $^2J_{CP}$ = 16 Hz, bipy), 138.8 (*s*, Ph), 136.3 (*d*, J_{CP} = 31 Hz, bipy), 132.9 (*d*, $^3J_{CP}$ = 2 Hz, Ph), 131.8 (*d*, $^2J_{CP}$ = 11 Hz, Ph), 129.7 (*s*, bipy), 129.3 (*s*, bipy), 127.8 (*d*, $^2J_{CP}$ = 7 Hz, Ph); $^{31}P\{^1H\}$ NMR (CD_3CN, 298 K, 121.4 MHz, δ [ppm]): 136.8 (*s*); $^{19}F\{^1H\}$ NMR (CD_3CN, 298 K, 282.2 Hz, δ [ppm]): -79.2 (*s*); IR (Nujol mull, NaCl plates, cm^{-1}): 1622 (m), 1480 (m), 1464 (s), 1457 (s), 1448 (s), 1377 (m), 1335 (m), 1254 (s), 1163 (s), 1100 (m), 1092 (m), 1071 (m), 1054 (m), 1045 (m), 1024 (s), 998 (m), 975 (w), 788 (w), 772 (w), 758 (w), 748 (w), 715 (m), 688 (w), 635 (s), 574 (s).

[PhP(^{t}Bu$_2$bipy)][OTf]$_2$ ([3^{t}Bu$_2$bipy]$^{2+}$; 10-4): To a rapidly stirring solution of $PhPCl_2$ (1.00 mmol, 0.179 g) and TMSOTf (2.00 mmol, 0.445 g) in 5 mL DCM, ^{t}Bu2bipy (1.00 mmol, 0.268 g) was added, producing a pale-yellow solution. The solution was stirred for 1 hr and then checked by $^{31}P\{^1H\}$ NMR spectroscopy. The solvent was removed under reduced pressure and washed with diethyl ether three times. The colourless powder product was crystallized in MeCN at -26 ˚C. Yield: 0.5936 g (88 %); Melting Point: 230 - 231 °C; ^1H NMR (CD_3CN, 298 K, 300 MHz, δ [ppm]): 9.20 – 9.17 (*m*, 4H, aromatic ^{t}Bu$_2$bipy), 8.33 (*dt*, 7 Hz, 6 Hz, 2H, aromatic ^{t}Bu$_2$bipy), 7.85 – 7.58 (*m*, 5H, Ph), 1.55 (*s*, 18H, ^{t}Bu); $^{13}C\{^1H\}$ NMR (CD_3CN, 298 K, 75.4 MHz, δ [ppm]): 177.4 (*s*, aromatic ^{t}Bu$_2$bipy), 146.2 (*d*, $^3J_{CP}$ = 4 Hz, aromatic ^{t}Bu$_2$bipy), 145.0 (*d*, $^2J_{CP}$ = 16 Hz, aromatic ^{t}Bu$_2$bipy), 138.4 (*s*, Ph), 135.9 (*d*, J_{CP} = 31 Hz, Ph), 131.6 (*d*, $^2J_{CP}$ = 10 Hz, Ph), 130.4 (*s*, aromatic ^{t}Bu$_2$bipy), 129.9 (*d*, $^3J_{CP}$ = 2 Hz, Ph), 125.4 (*d*, $^3J_{CP}$ = 4 Hz, aromatic ^{t}Bu$_2$bipy), 39.1 (*s*, ^{t}Bu), 30.4 (*s* ^{t}Bu); $^{31}P\{^1H\}$ NMR (CD_3CN, 298 K, 121.4 MHz, δ [ppm]): 133.8 (*s*); $^{19}F\{^1H\}$ NMR (CD_3CN, 298 K, 282.2 Hz, δ [ppm]): -79.2 (*s*); IR (Nujol mull, NaCl plates, cm^{-1}):1963 (w), 1703 (w), 1629 (s), 1542 (s), 1494 (s), 1466 (s), 1440 (s), 1279 (s), 1242 (s), 1224 (s), 1181 (s), 1077 (s), 1054 (s), 999 (m), 941 (m), 935 (m), 857 (m), 748 (m), 689 (m); E. A. for $C_{26}H_{29}F_6N_2O_6PS_2$ actual (calculated): C 45.97% (46.29%), H 4.42% (4.33%), N 4.05% (4.15%).

[PhP(DMAP)$_2$][OTf]$_2$ ([3DMAP]$^{2+}$; 10-3): To a rapidly stirring solution of $PhPCl_2$ (1.00 mmol, 0.179 g) and TMSOTf (2.00 mmol, 0.445 g) in 5 mL DCM, DMAP (4.00 mmol, 0.489 g) was added, producing a pale pink solution. The solution was stirred for 1 hr and then checked by $^{31}P\{^1H\}$ NMR spectroscopy. The solvent was removed under reduced pressure and washed with diethyl ether three times. The colourless powder product was crystallized from MeCN at -26 ˚C for 48 hr, yielding pale peach crystals. Yield: 0.4423 g (68 %); Melting Point: 159 – 161 °C; ^1H NMR (CD_2Cl_2, 298 K, 300 MHz, δ [ppm]): 8.32 – 8.29 (*m*, 4H, aromatic DMAP), 7.77 – 7.63 (*m*, 5H, Ph), 7.05 – 7.01 (*m*, 4H, aromatic DMAP), 3.30 (*broad s*, 12H, Me); $^{13}C\{^1H\}$ NMR (CD_2Cl_2, 298 K, 75.4 MHz, δ [ppm]): 158.7 (*s*, Ph), 144.3 (*d*, $^2J_{CP}$ = 19 Hz, Ph), 134.8 (*s*, aromatic DMAP), 132.6 (*s*, aromatic DMAP), 132.4 (*s*, aromatic DMAP), 131.4 (*d*, $^2J_{CP}$ = 7 Hz, Ph), 110.7 (*d*, $^3J_{CP}$ = 4 Hz, Ph), 41.7 (*s*, Me); $^{31}P\{^1H\}$ NMR (CD_2Cl_2, 298 K, 121.4 MHz, δ [ppm]): 121.03 (*s*); $^{19}F\{^1H\}$ NMR (CD_2Cl_2, 298 K, 282.2 Hz, δ [ppm]): -78.8 (*s*); IR (Nujol mull, NaCl plates, cm^{-1}): 1645 (s), 1579 (s), 1533 (s), 1507 (s), 1455 (s), 1406 (s), 1377 (s), 1342 (s), 1323 (s), 1258 (s), 1224 (s), 1169 (s), 1140 (s), 1061 (s), 1028 (s), 998 (s), 945 (m), 930 (m), 835 (s), 800 (s), 757 (s), 721 (m), 706 (s), 692 (s), 654 (m), 635 (m).

[PhP(SPCy$_3$)$_2$][OTf]$_2$ ([3SPCy$_3$]$^{2+}$; 11-3): To a rapidly stirring solution of $PhPCl_2$ (0.408 mmol, 0.073 g) and TMSOTf (0.816 mmol, 0.181 g) in 5 mL DCM, $SPCy_3$ (0.816 mmol, 0.255 g) was added, producing a colourless solution. The solution was stirred for 1 hr and then checked by $^{31}P\{^1H\}$ NMR spectroscopy and ^1H NMR spectroscopy. The solvent was removed under reduced pressure and washed with diethyl ether three times. The colourless powder product was crystallized from DCM layered with diethyl ether at room temperature. Yield: 0.2398 g (57 %); Melting Point: 188 - 190 °C; ^1H NMR (CD_3CN, 298 K, 300 MHz, δ [ppm]): 8.13 – 7.62 (*m*, 5H, Ph), 2.76 – 1.20 (*m*, 64H, Cy with CD_3CN included); $^{13}C\{^1H\}$ NMR (CD_3CN, 298 K, 75.4 MHz, δ [ppm]): 136.0 (*s*, Ph), 134.5 (*s*, Ph), 134.13 (*s*, Ph), 131.8 (*d*, J_{CP} = 10 Hz, Ph), 36.0 (*d*, J_{CP} = 29 Hz, Cy), 28.6 (*broad s*, Cy), 27.3 (*d*, J_{CP} = 13 Hz, Cy), 26.1 (*s*, Cy); $^{31}P\{^1H\}$ NMR (CD_3CN, 298 K, 121.4 MHz, δ [ppm]): 73.7 (*d*, $^2J_{PP}$ = 21 Hz), 61.5 (*t* ,$^2J_{PP}$ = 20 Hz) see figure 13; $^{19}F\{^1H\}$ NMR (CD_3CN, 298 K, 282.2 Hz, δ [ppm]): -79.2 (*s*); IR (Nujol mull, NaCl plates, cm^{-1}): 1580 (w), 1463 (s), 1454 (s), 1377 (m), 1366 (m), 1328 (w), 1301 (m), 1270 (s), 1257 (s), 1220 (m), 1182 (w), 1150 (s), 1086 (w), 1072 (w), 1044 (w), 1029 (s), 1002 (m), 994 (w), 921 (w), 896 (w), 854 (w), 825 (w), 812 (w), 761 (m), 753 (m), 740 (w), 723 (w), 700 (w), 636 (s).

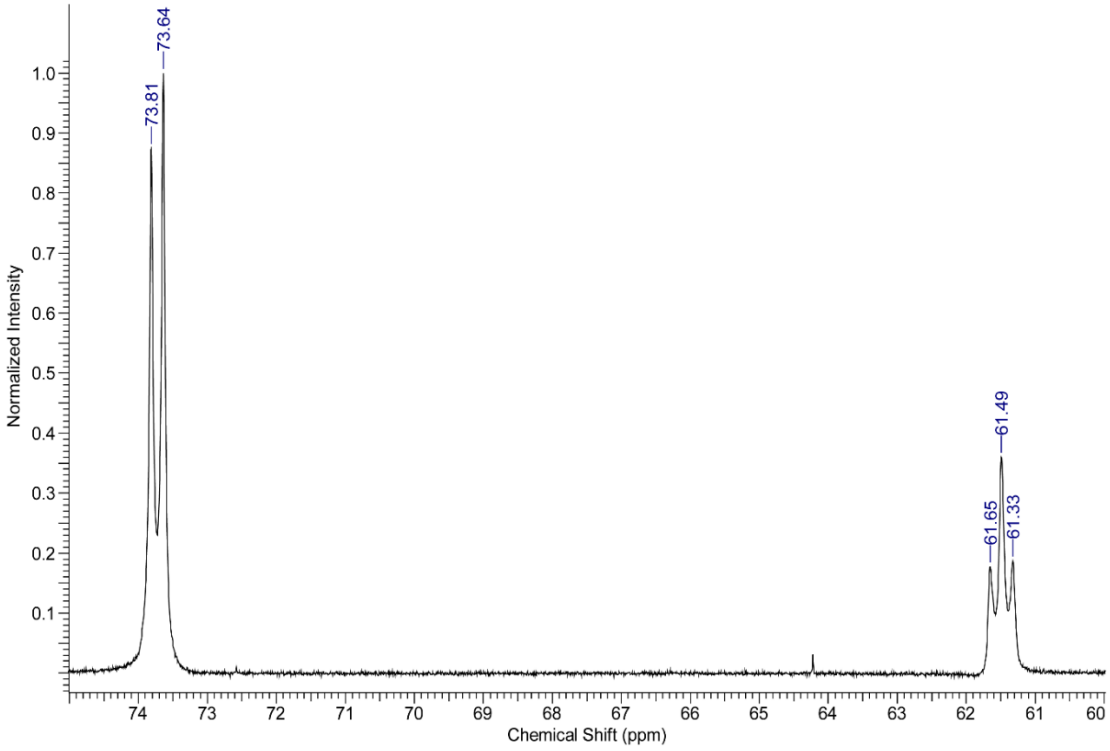

Figure 13. $^{31}P\{^1H\}$ NMR spectrum of **[3SPCy$_3$]$^{2+}$**

General procedure for Table 10-13: To a rapidly stirring mixture of Reagent A ($RPCl_2$) and Reagent B in 5 mL of solvent, Reagent C (L) was slowly added. The reaction was monitored by $^{31}P\{^1H\}$ NMR spectroscopy and if the NMR spectrum showed no change in the starting material chemical shift, the mixture was left to stir for an additional 1 hr, and then overnight if no change was observed after 1 hr. The solution was concentrated to about 2 mL, and then layered with 1 mL of diethyl ether and placed in the freezer at -25 °C for at least 48 hr, unless otherwise noted. Any recovered crystals are analyzed by $^{31}P\{^1H\}$ NMR, melting point, IR spectroscopy and x-ray diffraction.

Table 10. Syntheses of Dicationic Complexes using $PhPCl_2$, L = Nitrogen donating

Entry	Reagent B	Reagent C	Solvent	$^{31}P\{^1H\}$ NMR δ (ppm)	Assignment
1	4TMSOTf	^{t}Bu$_2$bipy	MeCN	133.8	**[3^{t}Bu$_2$bipy]$^{2+}$**
2	4TMSOTf	bipy	MeCN	136.6	**[3bipy]$^{2+}$**
3	4TMSOTf	4DMAP	DCM	121.3	**[3DMAP]$^{2+}$**
4	2TMSOTf	^{t}Bu$_2$bipy	DCM	133.9	**[3^{t}Bu$_2$bipy]$^{2+}$**
5	2TMSOTf	2Pico	DCM	-	-
6	2.5TMSOTf	1.5^{t}Bu$_2$bipy	DCM	134.0	**[3^{t}Bu$_2$bipy]$^{2+}$**
7	2.5TMSOTf	^{Me}PDI	DCM	34.1	**[3^{Me}PDI]$^{2+}$**
8	1.1TMSOTf	1.2^{Me}PDI	DCM	-	-
9	2.5TMSOTf	2.5^{dipp}DAB	DCM	49.3	**[3^{dipp}DAB]$^{2+}$**
10	2.5TMSOTf	BIAN	DCM	61.6	**[3BIAN]$^{2+}$**
11	^{ipr}PDI	2.5TMSOTf	DCM	-	-
12	2.5DMAP	2.5TMSOTf	DCM	134.3	**[3DMAP]$^{2+}$**
13	2.5TMSOTf	1.5^{t}Bu$_2$bipy	DCM	133.8	**[3^{t}Bu$_2$bipy]$^{2+}$**

Reactions were performed at room temperature and were stirred for 1 hr and then assessed by $^{31}P\{^1H\}$ NMR spectroscopy. Mixtures were stirred overnight if starting material was still present in the $^{31}P\{^1H\}$ NMR spectrum. Assignments of – indicate that the resulting compound cannot be determined/peak cannot be assigned.

Table 11. Syntheses of Dicationic Complexes using $PhPCl_2$, L = O, S, Se, or P donating

Entry	Reagent B	Reagent C	Solvent	$^{31}P\{^1H\}$ NMR δ (ppm)	Assignment
1	2TMSOTf	$2OPPh_3$	DCM	52.0	**Ph_3PO-TMS**
2	2TMSOTf	Ph_2S_2	DCM	109.1	**$[3Ph_2S_2]^{2+}$**
3	2TMSOTf	$2SPCy_3$	DCM	73.7 (*d*), 61.5 (*t*)	**$[3SPCy_3]^{2+}$**
4	2TMSOTf	$2Ph_3PS$	DCM	42.6	**Ph_3PS**
5	2TMSOTf	Triphos	DCM	-	-
6	{2AgOTf	$2OPPh_3$}	DCM	-	-
7	2TMSOTf	tdme	DCM	-	-
8	$SPPh_3$	2.5TMSOTf	DCM	43.1	**Ph_3PS-TMS**
9	2 $OPPh_3$	2AgOTf	DCM	-	-
10	$OPCy_3$	2.5TMSOTf	DCM	84.1	**Cy_3PO-TMS**
11	$SePCy_3$	2TMSOTf	DCM	127.8	**$[3SePCy_3]^{2+}$**
12	$2SePCy_3$	2TMSOTf	DCM	127.7	**$[3SePCy_3]^{2+}$**
13	2.5TMSOTf	$2.5SPCy_3$	DCM	73.5 (*d*), 59.6 (*t*)	**$[3SPCy_3]^{2+}$**
14	2.5TMSOTf	$2.5SePCy_3$	DCM	-	**$[3SePCy_3]^{2+}$**

Reactions were performed at room temperature and were stirred for 1 hr and then assessed by $^{31}P\{^1H\}$ NMR spectroscopy. Mixtures were stirred overnight if starting material was still present in the $^{31}P\{^1H\}$ NMR spectrum. Assignments of – indicate that the resulting compound cannot be determined/peak cannot be assigned.

Table 12. Syntheses of Dicationic Complexes using Ph_2PCl

Entry	Reagent B	Reagent C	Solvent	$^{31}P\{^1H\}$ NMR δ (ppm)	Assignment
1	4TMSOTf	bipy	MeCN	-	-
2	4TMSOTf	DMAP	MeCN	88	**Ph_2P-DMAP**[6]
3	4TMSOTf	bipy	MeCN	25.6	**Ph_2P(bipy)**
4	4TMSOTf	bipy	DCM	-	-

Reactions were performed at room temperature and were stirred for 1 hr and then assessed by $^{31}P\{^1H\}$ NMR spectroscopy. Mixtures were stirred overnight if starting material was still present in the $^{31}P\{^1H\}$ NMR spectrum. Assignments of – indicate that the resulting compound cannot be determined/peak cannot be assigned.

Table 13. Syntheses of Dicationic Complexes where R = Cy, ^{t}Bu, or (^{i}Pr$_2$)N (in DCM)

Entry	Reagent A	Reagent B	Reagent C	$^{31}P\{^1H\}$ NMR δ (ppm)	Assignment
1	$CyPCl_2$	2TMSOTf	^{t}Bu$_2$bipy	164.4	**[CyP(^{t}Bu$_2$bipy)]$^{2+}$**
2	$CyPCl_2$	2.5DMAP	2.5TMSOTf	195.5	**$CyPCl_2$**
3	^{t}BuPCl$_2$	2.5DMAP	2.5TMSOTf	158.7	**[DMAP-TMS]$^+$**
4	(^{i}Pr$_2$N)PCl$_2$	2TMSOTf	^{t}Bu$_2$bipy	128.7	**[(^{i}Pr$_2$N)P(^{t}Bu$_2$bipy)]$^{2+}$**

Reactions were performed at room temperature and were stirred for 1 hr and then assessed by $^{31}P\{^1H\}$ NMR spectroscopy. Mixtures were stirred overnight if starting material was still present in the $^{31}P\{^1H\}$ NMR spectrum. Assignments of – indicate that the resulting compound cannot be determined/peak cannot be assigned.

Chapter 4. Summary and Conclusions

Coordination chemistry usually applies to transition metals, but has recently been extended to the *p*-block elements. However, Lewis acidic complexes with the relatively light pnictogen atom phosphorus have not been extensively explored, due to its relatively small atomic radii. To enhance the Lewis acidity at the phosphorus centre, a cationic charge can be introduced by abstracting an anionic substituent, providing more opportunities for new reactivity. The presence of a stereochemically active lone pair at the acceptor site also introduces new reactivity patterns as the complexes can potentially behave as ambiphilic species. The developing library of main group polycationic complexes has been expanded, by the assessment of the $[P(^tBu_2bipy)_2][OTf]_3$ tricationic complex, **[1]$^{3+}$**, and by the isolation and full characterisation of four new $[PhP]^{2+}$ centred dicationic complexes, **[3DMAP]$^{2+}$**, **[3SPCy$_3$]$^{2+}$**, **[3^{t}Bu$_2$bipy]$^{2+}$**, and **[3bipy]$^{2+}$**. In the future, it can be envisaged that these compounds can be used for small molecule activation, catalysis, and as precursors to new materials.

Chapter 2 showcases how **[1]$^{3+}$** can react with multiple reagents and can act as a Lewis acid and as a Lewis base. Where **[1]$^{3+}$** has been shown to activate C-H and H-H bonds, experiments with other small molecules such as NBN and NBD were attempted. Those reactions along with MeOTf, showcases that new complexes can be formed with **[1]$^{3+}$**, based on $^{31}P\{^1H\}$ NMR spectroscopy, although electrophilic reactions with trialkyl chalcogen oxides proved to be less fruitful. This reactivity study showed that **[1]$^{3+}$** can be oxidized (using SO_2Cl_2) and can also be reduced (using Mg or Zn), allowing it to be a diverse compound to be used in future reactions, such as catalysis. Although no crystallographic data was obtained, the presence of a new chemical shift in the $^{31}P\{^1H\}$ NMR spectrum indicates the presence of the proposed product **[2]$^{5+}$**. However, the reduction by-product $[Mg(^tBu_2bipy)_2][OTf]_2$ was isolated, indicating the potential synthesis of **[2]$^{5+}$**. With further development, these highly Lewis acidic complexes have possible small molecule activation and catalytic applications.

Chapter 3 showcases how $[PhP]^{2+}$ complexes can be easily synthesised in an elegant one-pot reaction, and coupled with the fact they still retain their lone pair, the newly synthesised compounds show a promising future in reactivity studies similar to $\mathbf{[1]^{3+}}$, as discussed in **Chapter 2**. More exploration is required in order to expand this library of $[RP]^{2+}$ complexes; and reactivity investigations would be necessary. It would not be improbable to think that in the future these complexes could be used in small molecule activation and even in catalysis with their ambiphilic nature.

Chapter 5. Future Work

The reactivity of **[1]$^{3+}$** has been extensively tested, resulting in new compounds as observed by $^{31}P\{^{1}H\}$ NMR spectroscopy measurements. The next step would be to successfully crystalize these compounds, and test their reactivity. Preliminary experiments have been done to replace the triflate anion with other weakly coordinating anions such as hexafluorophosphate (PF_6^-) and *Tetrakis*[3,5-*bis*(trifluoromethyl)phenyl]borate ([{3,5-$(CF_3)_2C_6H_3\}_4B]^-$, in hopes to increase the crystallization potential, but to no avail. Where the mono-ligand $[P(^tBu_2bipy)][OTf]_3$ complex has been synthesised previously in the Burford Group[65], it would be interesting to see if there are any similarities in its reactivity when compared to **[1]$^{3+}$**. Reactions with SO_2Cl_2, Mg, MeOTf, and some ring compounds like NBN and NBD, would be a good starting point for investigation for the comparison with **[1]$^{3+}$**. Experiments with other small molecules such as CO, CO_2, N_2, and NO would also be interesting to investigate, where **[1]$^{3+}$** has already been shown to activate H_2 and 1,4-cyclohexadiene.

The continuous development of new P centred tricationic complexes is currently underway, with the successful isolation of $[P(BimEt_3)][OTf]_3$ (**Figure 6**; **6-14** in **Table 6**.) This complex still needs to be fully characterized and reproducibility experiments still need to be conducted, however, preliminary work has been done to synthesise other Pn centred complexes stabilized with $BimEt_3$, and other multidentate nitrogen ligands, such as 2,6-pyridine(diimine) (^{Me}PDI), *bis*(aryl-imino)acenaphthene (BIAN), and 1,4-diaza-1,3-butadiene (DAB) (as seen in **Table 6**).

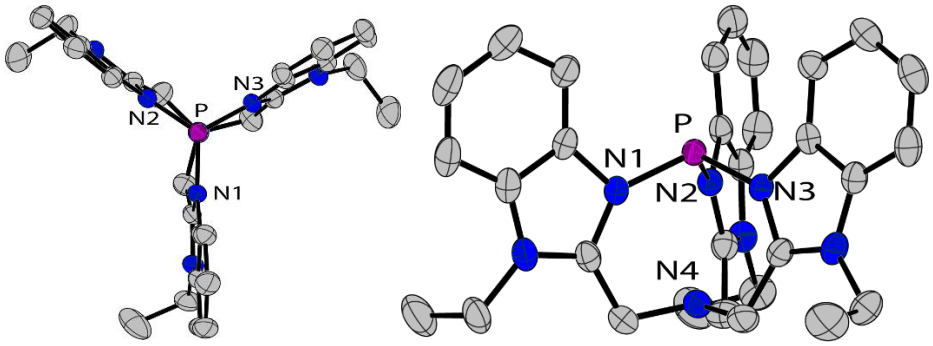

Figure 6. Solid-state structure of [P(BimEt$_3$)][OTf]$_3$

Where the newly synthesised dicationic complex, [PhP(^{t}Bu$_2$bipy)][OTf]$_2$ shares similarities with the extensively tested **[1]**$^{3+}$ tricationic complex, it would be interesting to compare their reactivities. Reactions with SO_2Cl_2, Mg, MeOTf, and some ring compounds, like NBN and NBD, would provide a good preliminary assessment of the reactivity of [PhP(^{t}Bu$_2$bipy)][OTf]$_2$. Performing these experiments with the other newly synthesised dicationic complexes would be beneficial as well (**Scheme 41**).

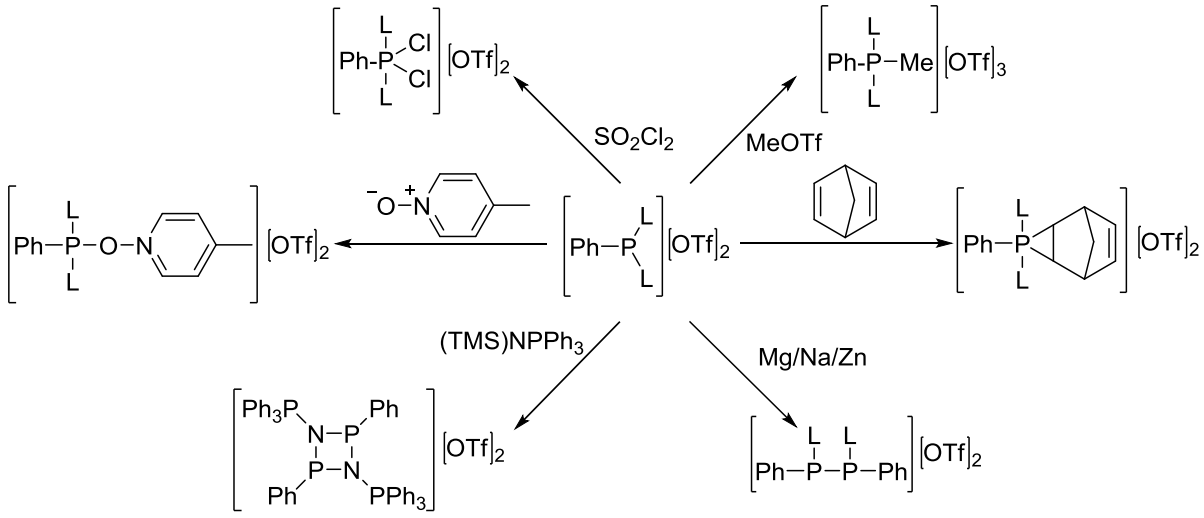

Scheme 41. Potential reactions of **[3L]**$^{2+}$ with various reagents

Where dicationic complexes have ambiphilic nature, catalytic investigations are of high interest. More exploration is needed for the expansion of the of $[RP]^{2+}$ library, especially with chalcogens, where no other example of a *bis*(tricyclohexylphosphine chalcogenide) pnictogen centred cationic complex exist. Preliminary experiments have been performed in the attempt to synthesise new chalcogen stabilizing dicationic complexes, such as $[PhP(SPPh_3)_2][OTf]_2$, $[PhP(OPPh_3)_2][OTf]_2$, and of $[PhP(SePCy_3)_2][OTf]_2$ which has been recently isolated (**Figure 7**; **11-14** in **Table 11**), but still needs to be fully characterized and reproducibility experiments still need to be conducted.

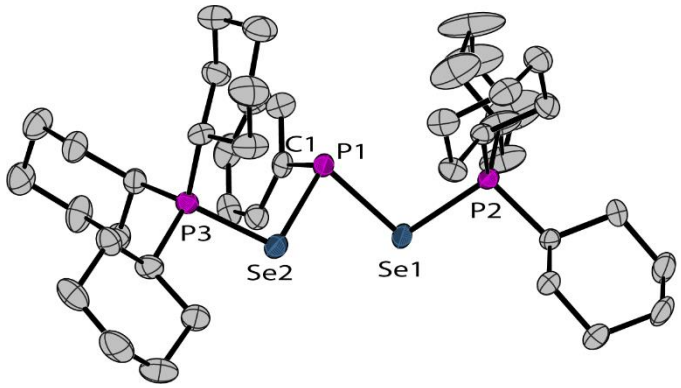

Figure 7. Solid-state structure of $[PhP(SePCy_3)_2][OTf]_2$

Bibliography

1 K. Bowman-James, *Acc. Chem. Res.*, 2005, **38**, 671–678.

2 M. I. Bruce, M. J. Liddell, C. A. Hughes, B. W. Skelton and A. H. White, *J. Organomet. Chem.*, 1988, **347**, 157–180.

3 P. P. Power, *Nature*, 2010, **463**, 171–177.

4 N. C. Norman and N. L. Pickett, *Coord. Chem. Rev.*, 1995, **145**, 27–54.

5 S. S. Chitnis, N. Burford and M. J. Ferguson, *Angew. Chem. Int. Ed.*, 2013, **52**, 2042–2045.

6 N. Burford, P. Losier, A. D. Phillips, P. J. Ragogna and T. S. Cameron, *Inorg. Chem.*, 2003, **42**, 1087–1091.

7 N. Burford, H. A. Spinney, M. J. Ferguson and R. McDonald, *Chem. Commun.*, 2004, **2**, 2696–2697.

8 N. Burford, T. Stanley Cameron, K. N. Robertson, A. D. Phillips and H. A. Jenkins, *Chem. Commun.*, 2000, 2087–2088.

9 N. Burford, A. D. Phillips, H. A. Spinney, M. Lumsden, U. Werner-Zwanziger, M. J. Ferguson and R. McDonald, *J. Am. Chem. Soc.*, 2005, **127**, 3921–3927.

10 N. Burford and P. J. Ragogna, *J. Chem. Soc. Dalton Trans.*, 2002, 4307–4315.

11 A. P. M. Robertson, P. A. Gray and N. Burford, *Angew. Chemie Int. Ed.*, 2014, **53**, 6050–6069.

12 B. D. Ellis and C. L. B. Macdonald, *Coord. Chem. Rev.*, 2007, **251**, 936–973.

13 G. M. Omietanski and H. H. Sisler, *J. Am. Chem. Soc.*, 1956, **78**, 1211–1213.

14 H. H. Sisler and S. R. Jain, *Inorg. Chem.*, 1968, **7**, 104–107.

15 R. M. Kren and H. H. Sisler, *Inorg. Chem.*, 1970, **9**, 836–839.

16 H. H. Sisler and C. Stratton, *Inorg. Chem.*, 1966, **5**, 2003–2008.

17 S. R. Jain and H. H. Sisler, *Inorg. Chem.*, 1968, **7**, 2204–2207.

18 A. Boardman, R. W. H. Small and I. J. Worrall, *Inorg. Chim. Acta*, 1986, **121**, L35–L36.

19 D. R. Lide, Ed., *CRC Handbook of Chemistry and Physics*, CRC Press, Boca Raton, 85th edn., 2004.

20 S. S. Chitnis, B. Peters, E. Conrad, N. Burford, R. McDonald and M. J. Ferguson, *Chem. Commun.*, 2011, **47**, 12331–12333.

21 F. Huber, H. Preut, G. Alonzo, N. Bertazzi, *Inorg. Chim. Acta*, 1985, **102**, 181–186.

22 N. L. Kilah, S. Petrie, R. Stranger, J. W. Wielandt, A. C. Willis and S. B. Wild, *Organometallics*, 2007, **26**, 6106–6113.

23 E. Conrad, N. Burford, R. McDonald and M. J. Ferguson, *J. Am. Chem. Soc.*, 2009, **131**, 5066–5067.

24 C. J. Carmalt, L. J. Farrugia and N. C. Norman, *J. Chem. Soc. Dalton Trans.*, 1996, 443–454.

25 C. J. Carmalt, N. C. Norman, A. G. Orpen and S. E. Stratford, *J. Organomet. Chem.*, 1993, **460**, C22–C24.

26 C. J. Carmalt, L. J. Farrugia and N. C. Norman, *J. Chem. Soc. Dalton Trans.*, 1996, 455–459.

27 W. Clegg, L. J. Farrugia, A. McCamley, N. C. Norman, A. G. Orpen, N. L. Pickett and S. E. Stratford, *J. Chem. Soc., Dalton Trans.*, 1993, 2579–2587.

28 E. Conrad, N. Burford, R. McDonald and M. J. Ferguson, *Chem. Commun.*, 2010, **46**, 4598–4600.

29 M. A. Tershansy, A. M. Goforth, M. D. Smith and H.-C. zur Loye, *J. Chem. Crystallogr.*, 2008, **38**, 453–459.

30 R. Weiss and S. Engel, *Synthesis*, 1991, 1077–1079.

31 G. Bouhadir, R. W. Reed, R. Réau and G. Bertrand, *Heteroat. Chem.*, 1995, **6**, 371–375.

32 J. J. Weigand, K. O. Feldmann, A. K. C. Echterhoff, A. W. Ehlers and K. Lammertsma, *Angew. Chem. Int. Ed.*, 2010, **49**, 6178–6181.

33 L. Gu, G. Gopakumar, P. Gualco, W. Thiel and M. Alcarazo, *Chem. Eur. J.*, 2014, **20**, 8575–8578.

34 J. Petuškova, M. Patil, S. Holle, C. W. Lehmann, W. Thiel and M. Alcarazo, *J. Am. Chem. Soc.*, 2011, **133**, 20758–20760.

35 S. S. Chitnis, A. P. M. Robertson, N. Burford, B. O. Patrick, R. McDonald and M. J. Ferguson, *Chem. Sci.*, 2015, **6**, 6545–6555.

36 M. Zeldin, P. Mehta and W. D. Vernon, *Inorg. Chem.*, 1979, **18**, 463–466.

37 S. S. Chitnis, P-P and P-Sb Coordination Chemistry, PhD Dissertation, University of Victoria, Victoria, 2015.

38 S. E. Pipko, L. V Bezgubenko, A. D. Sinitsa, E. B. Rusanov, E. G. Kapustin, M. I. Povolotskii and V. V Shvadchak, *Heteroat. Chem.*, 2008, **19**, 171–177.

39 K. B. Dillon, R. N. Reeve and T. C. Waddington, *J. Chem. Soc. Dalton Trans.*, 1977, 2382–2388.

40 P. Pyykkö and M. Atsumi, *Chem. Eur. J.*, 2009, **15**, 186–197.

41 S. Alvarez, *Dalton Trans.*, 2013, **42**, 8617–8636.

42 J. E. McDonough, A. Mendiratta, J. J. Curley, G. C. Fortman, S. Fantasia, C. C. Cummins, E. V. Rybak-Akimova, S. P. Nolan and C. D. Hoff, *Inorg. Chem.*, 2008, **47**, 2133–2141.

43 G. M. Sheldrick, *Acta Crystallogr. Sect. A Found. Crystallogr.*, 2008, **64**, 112–122.

44 C. A. Dyker and N. Burford, *Chem. Asian J.*, 2008, **3**, 28–36.

45 A. Schmidpeter, S. Lochschmidt, K. Karaghiosoff and W. S. Sheldrick, *J. Chem. Soc. Chem. Commun.*, 1985, 1447–1448.

46 J. J. Weigand, N. Burford, A. Decken and A. Schulz, *Eur. J. Inorg. Chem.*, 2007, **3**, 4868–4872.

47 K. B. Dillon, A. E. Goeta, J. A. K. Howard, P. K. Monks, H. J. Shepherd and A. L. Thompson, *Dalton Trans.*, 2008, 1144–1149.

48 R. Bashforth, A. J. Boyall, P. K. Coffer (née Monks), K. B. Dillon, A. E. Goeta, J. A. K. Howard, A. M. Kenwright, M. R. Probert, H. J. Shepherd and A. L. Thompson, *Dalton Trans.*, 2012, **41**, 1165–1172.

49 Á. Kozma, J. Rust and M. Alcarazo, *Chem. Eur. J.*, 2015, **21**, 10829–10834.

50 J. J. Weigand, K. O. Feldmann and F. D. Henne, *J. Am. Chem. Soc.*, 2010, **132**, 16321–16323.

51 K. Schwedtmann, S. Schulz, F. Hennersdorf, T. Strassner, E. Dmitrieva and J. J. Weigand, *Angew. Chem. Int. Ed.*, 2015, **54**, 11054–11058.

52 K. Schwedtmann, M. H. Holthausen, K. O. Feldmann and J. J. Weigand, *Angew. Chem. Int. Ed.*, 2013, **52**, 14204–14208.

53 M. Azouri, J. Andrieu, M. Picquet and H. Cattey, *Inorg. Chem.*, 2009, **48**, 1236–1242.

54 V. G. Nenajdenko, N. E. Shevchenko, E. S. Balenkova and I. V. Alabugin, *Chem. Rev.*, 2003, **103**, 229–282.

55 J. J. Weigand, S. D. Riegel, N. Burford and A. Decken, *J. Am. Chem. Soc.*, 2007, **129**, 7969–7976.

56 P. A. Gray, Y. Carpenter, N. Burford and R. McDonald, *Dalton Trans.*, 2016, **45**, 2124–2129.

57 S. S. Chitnis, A. P. M. Robertson, N. Burford, J. J. Weigand and R. Fischer, *Chem. Sci.*, 2015, **6**, 2559–2574.

58 J. L. Dutton and P. J. Ragogna, *Coord. Chem. Rev.*, 2011, **255**, 1414–1425.

59 M. Q. Y. Tay, Y. Lu, R. Ganguly and D. Vidovič, *Angew. Chem. Int. Ed.*, 2013, **52**, 3132–3135.

60 Z. B. Maksic and B. Kovacevic, *J. Chem. Soc. Trans.*, 1999, **2**, 2623–2629.

61 K. A. Kerr, P. M. Boorman, B. S. Misener and J. G. H. van Roode, *Can. J. Chem.*, 1977, **55**, 3081–3085.

62 K. L. Bamford, A. P. M. Robertson, H. A. Jenkins, B. O. Patrick and N. Burford, *Can. J. Chem.*, 2015, **93**, 375–379.

63 W. Levason, M. E. Light, S. Maheshwari, G. Reid and W. Zhang, *Dalton Trans.*, 2011, **40**, 5291–5297.

64 K. Tani, K. Matsuyama, S. Kato, K. Yamada and H. Mifune, *Bull. Chem. Soc. Jpn.*, 2000, **73**, 1243–1252.

65 K. Vos, ^{31}P NMR Spectroscopic Study of a Bipyridine Stabilized Phosphorus Trication, BSc. Thesis, University of Victoria, Vicotira, 2015

Appendix

Crystallographic Data

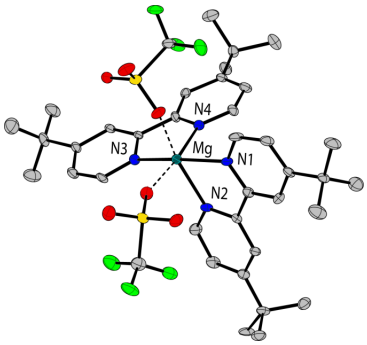

Collected by	Dr. Brian Patrick (UBC)
Empirical formula	$C_{41}H_{48}N_4P_3F_{15}O_{15}S_5Mg$
Formula weight	1399.35
Temperature/K	296.15
Crystal system	monoclinic
Space group	$P2_1/n$
a/Å	10.790(3)
b/Å	20.582(6)
c/Å	18.224(5)
α/°	90
β/°	90.409(5)
γ/°	90
Volume/Å^3	4047.3(19)
Z	1
ρ_{calc}g/cm^3	0.574
μ/mm^{-1}	0.146
F(000)	714.0
Crystal size/mm^3	0.25 × 0.15 × 0.15
Radiation	MoKα (λ = 0.71073)
2Θ range for data collection/°	2.984 to 56.796
Index ranges	$-14 \leq h \leq 14$, $-27 \leq k \leq 26$, $-24 \leq l \leq 24$
Reflections collected	56360
Independent reflections	10020 [R_{int} = 0.0689, R_{sigma} = 0.0714]
Data/restraints/parameters	10020/3/529
Goodness-of-fit on F^2	1.133
Final R indexes [I>=2σ (I)]	R_1 = 0.1507, wR_2 = 0.3879
Final R indexes [all data]	R_1 = 0.1747, wR_2 = 0.4070
Largest diff. peak/hole / e Å^{-3}	1.60/-1.05

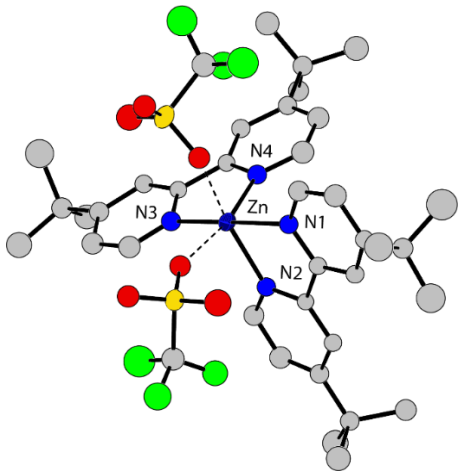

Collected by	Dr. Robert McDonald & Dr. Michael J. Ferguson (UofA)
Empirical formula	$C_{22}H_{16}F_6N_4O_6S_2Zn$
Formula weight	675.88
Temperature/K	193(2)
Crystal system	monoclinic
Space group	$P2_1/n$
a/Å	10.802(2)
b/Å	21.001(4)
c/Å	18.252(4)
α/°	90
β/°	90.10(3)
γ/°	90
Volume/Å^3	4140.7(14)
Z	4
ρ_{calc}g/cm^3	1.084
μ/mm^{-1}	0.751
F(000)	1360.0
Crystal size/mm^3	? × ? × ?
Radiation	MoKα (λ = 0.71073)
2Θ range for data collection/°	4.24 to 55.308
Index ranges	$-14 \leq h \leq -1$, $-6 \leq k \leq 22$, $-14 \leq l \leq 11$
Reflections collected	2908
Independent reflections	2515 [R_{int} = 0.0310, R_{sigma} = 0.0468]
Data/restraints/parameters	2515/0/244
Goodness-of-fit on F^2	1.051
Final R indexes [I>=2σ (I)]	R_1 = 0.0724, wR_2 = 0.2000
Final R indexes [all data]	R_1 = 0.0946, wR_2 = 0.2135
Largest diff. peak/hole / e Å^{-3}	0.39/-0.32
Completeness %	26.07

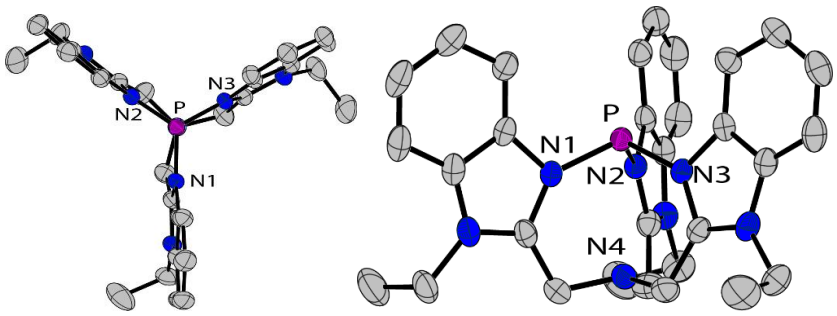

Collected by	Dr. Robert McDonald & Dr. Michael J. Ferguson (UofA)
Empirical formula	$C_{39}H_{42}N_{10}O_9F_9PS_3$
Formula weight	1092.97
Temperature/K	193.15
Crystal system	triclinic
Space group	P-1
a/Å	10.9002(19)
b/Å	11.0131(19)
c/Å	20.503(4)
α/°	81.471(2)
β/°	83.157(2)
γ/°	89.063(2)
Volume/Å^3	2416.7(7)
Z	2
ρ_{calc}g/cm^3	1.502
μ/mm^{-1}	0.284
F(000)	1124.0
Crystal size/mm^3	0.429 × 0.246 × 0.188
Radiation	MoKα (λ = 0.71073)
2Θ range for data collection/°	3.74 to 55.052
Index ranges	$-14 \leq h \leq 14$, $-14 \leq k \leq 14$, $-26 \leq l \leq 26$
Reflections collected	20626
Independent reflections	11048 [R_{int} = 0.0313, R_{sigma} = 0.0463]
Data/restraints/parameters	11048/0/672
Goodness-of-fit on F^2	1.047
Final R indexes [I>=2σ (I)]	R_1 = 0.0617, wR_2 = 0.1664
Final R indexes [all data]	R_1 = 0.0823, wR_2 = 0.1812
Largest diff. peak/hole / e Å^{-3}	0.96/-0.58

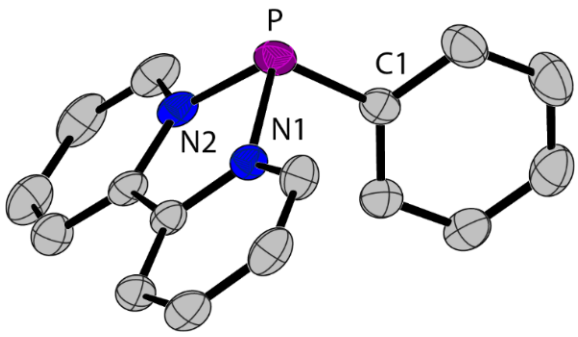

Collected by	Dr. Robert McDonald & Dr. Michael J. Ferguson (UofA)
Empirical formula	$C_{18}H_{13}N_2O_6F_6PS_2$
Formula weight	562.39
Temperature/K	173.15
Crystal system	triclinic
Space group	P-1
a/Å	7.3772(2)
b/Å	11.0469(3)
c/Å	14.8136(5)
α/°	74.9952(18)
β/°	77.2568(15)
γ/°	85.2235(14)
Volume/Å^3	1136.91(6)
Z	2
ρ_{calc}g/cm^3	1.643
μ/mm^{-1}	3.625
F(000)	568.0
Crystal size/mm^3	0.441 × 0.2 × 0.062
Radiation	CuKα (λ = 1.54178)
2Θ range for data collection/°	6.314 to 147.788
Index ranges	$-9 \leq h \leq 9$, $-13 \leq k \leq 13$, $-18 \leq l \leq 18$
Reflections collected	7962
Independent reflections	4427 [R_{int} = 0.0409, R_{sigma} = 0.0490]
Data/restraints/parameters	4427/0/316
Goodness-of-fit on F^2	1.084
Final R indexes [I>=2σ (I)]	R_1 = 0.0503, wR_2 = 0.1404
Final R indexes [all data]	R_1 = 0.0550, wR_2 = 0.1447
Largest diff. peak/hole / e Å^{-3}	0.75/-0.56

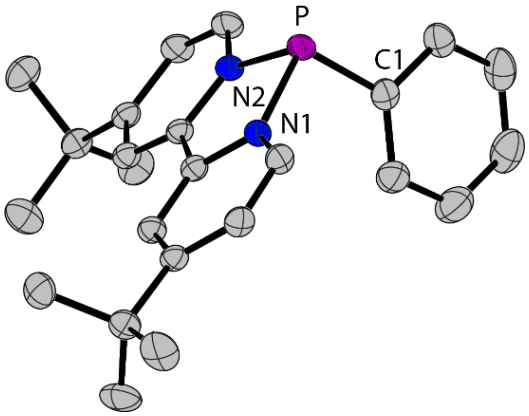

Collected by	Dr. Robert McDonald & Dr. Michael J. Ferguson (UofA)
Empirical formula	$C_{26}H_{29}N_2O_6F_6PS_2$
Formula weight	674.60
Temperature/K	173.15
Crystal system	triclinic
Space group	P-1
a/Å	10.3407(7)
b/Å	10.9356(7)
c/Å	14.1649(9)
α/°	109.229(3)
β/°	97.623(3)
γ/°	93.345(2)
Volume/Å^3	1490.12(17)
Z	2
ρ_{calc}g/cm^3	1.504
μ/mm^{-1}	2.863
F(000)	696.0
Crystal size/mm^3	0.402 × 0.335 × 0.33
Radiation	CuKα (λ = 1.54178)
2Θ range for data collection/°	6.696 to 148.152
Index ranges	$-12 \leq h \leq 12$, $-13 \leq k \leq 13$, $-17 \leq l \leq 17$
Reflections collected	10609
Independent reflections	5791 [R_{int} = 0.0260, R_{sigma} = 0.0334]
Data/restraints/parameters	5791/0/388
Goodness-of-fit on F^2	1.052
Final R indexes [I>=2σ (I)]	R_1 = 0.0378, wR_2 = 0.1057
Final R indexes [all data]	R_1 = 0.0393, wR_2 = 0.1072
Largest diff. peak/hole / e Å^{-3}	0.49/-0.41

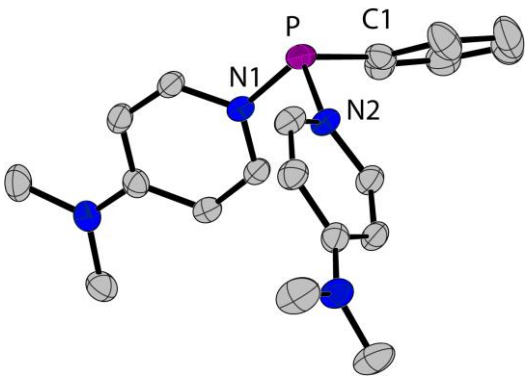

Collected by	Dr. Robert McDonald & Dr. Michael J. Ferguson (UofA)
Empirical formula	$C_{29}H_{35}N_6O_6F_6PS_2$
Formula weight	772.72
Temperature/K	173.15
Crystal system	orthorhombic
Space group	Fdd2
a/Å	20.5652(4)
b/Å	34.7966(7)
c/Å	16.2609(3)
α/°	90
β/°	90
γ/°	90
Volume/Å^3	11636.3(4)
Z	16
ρ_{calc}g/cm^3	1.764
μ/mm^{-1}	3.066
F(000)	6400.0
Crystal size/mm^3	0.338 × 0.25 × 0.23
Radiation	CuKα (λ = 1.54178)
2Θ range for data collection/°	7.382 to 145.022
Index ranges	$-25 \leq h \leq 25$, $-42 \leq k \leq 42$, $-20 \leq l \leq 19$
Reflections collected	19943
Independent reflections	5724 [R_{int} = 0.0167, R_{sigma} = 0.0165]
Data/restraints/parameters	5724/1/374
Goodness-of-fit on F^2	1.078
Final R indexes [I>=2σ (I)]	R_1 = 0.0513, wR_2 = 0.1527
Final R indexes [all data]	R_1 = 0.0515, wR_2 = 0.1529
Largest diff. peak/hole / e Å^{-3}	1.64/-0.46
Flack parameter	0.023(3)

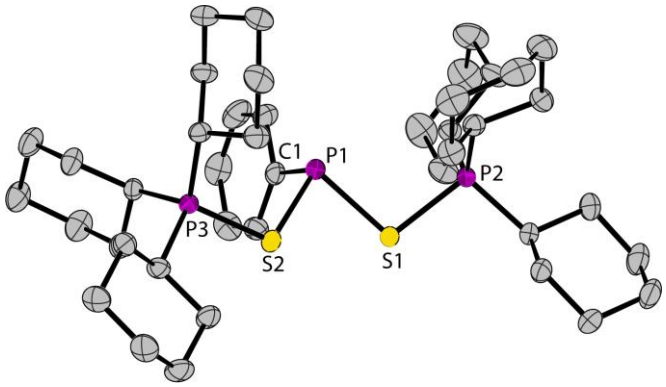

Collected by	Dr. Robert McDonald & Dr. Michael J. Ferguson (UofA)
Empirical formula	$C_{44}H_{71}F_6O_6P_3S_4$
Formula weight	1031.15
Temperature/K	173.15
Crystal system	orthorhombic
Space group	$Pca2_1$
a/Å	19.3394(6)
b/Å	10.6524(4)
c/Å	24.1489(8)
α/°	90
β/°	90
γ/°	90
Volume/Å^3	4974.9(3)
Z	4
ρ_{calc}g/cm^3	1.377
μ/mm^{-1}	3.243
F(000)	2184.0
Crystal size/mm^3	0.334 × 0.3 × 0.292
Radiation	CuKα (λ = 1.54184)
2Θ range for data collection/°	7.322 to 148.064
Index ranges	$-24 \leq h \leq 24$, $-12 \leq k \leq 10$, $-30 \leq l \leq 30$
Reflections collected	174874
Independent reflections	9890 [R_{int} = 0.0431, R_{sigma} = 0.0185]
Data/restraints/parameters	9890/1/568
Goodness-of-fit on F^2	0.998
Final R indexes [I>=2σ (I)]	R_1 = 0.0230, wR_2 = 0.0616
Final R indexes [all data]	R_1 = 0.0231, wR_2 = 0.0617
Largest diff. peak/hole / e Å^{-3}	0.22/-0.32
Flack parameter	0.021(2)

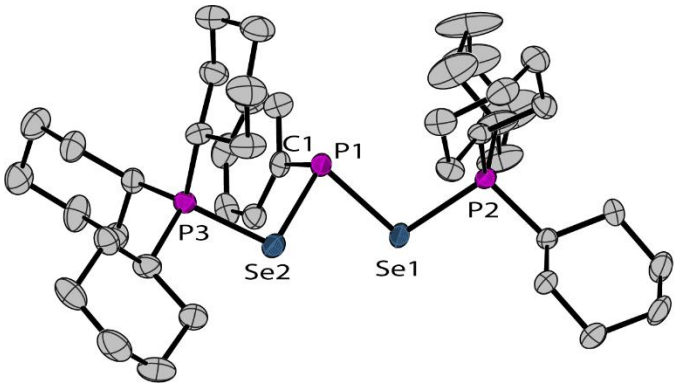

Collected by	Dr. Robert McDonald & Dr. Michael J. Ferguson (UofA)
Empirical formula	$C_{44}H_{71}O_6F_6P_3S_2Se_2$
Formula weight	1124.95
Temperature/K	193.15
Crystal system	orthorhombic
Space group	$Pca2_1$
a/Å	19.1271(10)
b/Å	21.3744(11)
c/Å	24.5753(12)
α/°	90
β/°	90
γ/°	90
Volume/Å^3	10047.1(9)
Z	8
ρ_{calc}g/cm^3	1.487
μ/mm^{-1}	1.717
F(000)	4656.0
Crystal size/mm^3	0.438 × 0.332 × 0.25
Radiation	MoKα (λ = 0.71073)
2Θ range for data collection/°	2.858 to 55.046
Index ranges	$-24 \leq h \leq 24$, $-27 \leq k \leq 27$, $-31 \leq l \leq 31$
Reflections collected	82438
Independent reflections	23072 [R_{int} = 0.0554, R_{sigma} = 0.0578]
Data/restraints/parameters	23072/1/1136
Goodness-of-fit on F^2	1.006
Final R indexes [I>=2σ (I)]	R_1 = 0.0399, wR_2 = 0.0822
Final R indexes [all data]	R_1 = 0.0582, wR_2 = 0.0890
Largest diff. peak/hole / e Å^{-3}	1.30/-0.93
Flack parameter	-0.005(6)